High-resolution climate projections for South Asia to inform climate impacts and adaptation studies in the Ganges-Brahmaputra-Meghna and Mahanadi deltas

Tamara Janes[1], Fintan McGrath[1], Ian Macadam[1], Richard Jones[1,2]

[1] Met Office Hadley Centre, Fitzroy Road, Exeter, UK

[2] Oxford University School of Geography and Environment, Dyson Perrins Building, South Parks Road, Oxford, UK

Corresponding author: Tamara Janes, Met Office Hadley Centre, Fitzroy Road, Exeter, UK, EX1 3PB, tamara.janes@metoffice.gov.uk.

KEY WORDS: regional climate modelling, monsoon dynamics, climate change

ABSTRACT

Climate impacts and adaptation studies often use output from impact models that require data representing future climates at a resolution greater than can be provided by Global Climate Models (GCMs). This paper describes the use of Regional Climate Model (RCM) simulations to generate high-resolution future climate information for assessing climate impacts in the Ganges-Brahmaputra-Meghna (GBM) and Mahanadi deltas as part of the DECCMA project. In this study, three different GCMs (HadGEM2-ES, CNRM-CM5 and GFDL-CM3), all using a single scenario for future greenhouse forcing of the atmosphere (RCP 8.5), were downscaled to a horizontal resolution of 25km over south Asia using the HadRM3P RCM. These three GCMs were selected based on ability to represent key climate processes over south Asia and ability to sample a range of regional climate change responses to greenhouse gas forcing. RCM simulations of temperature, precipitation, and lower level (850 hPa) atmospheric circulation in the monsoon season (June, July, August, September – JJAS) were compared with observational datasets and their respective driving GCMs to ensure large-scale consistency. Although there are some biases in the RCM simulations, these comparisons indicate that the RCMs are able to simulate realistically aspects of the observed climate of South Asia, such as the monsoon circulation and associated precipitation that are key for informing downstream impacts and adaptation studies. Simulated future temperature and precipitation changes on seasonal and daily timescales suggest increases in both temperature and precipitation across all three models during the monsoon season, with an increase in the amount of extremely heavy precipitation over the GBM and Mahanadi basins. Despite different driving conditions, these results are consistent across all three RCM simulations, providing a level of confidence in the magnitudes and spatial characteristics of temperature and precipitation projections for South Asia.

1. INTRODUCTION

Many delta regions of South Asia are densely populated and heavily reliant on agriculture for livelihoods and wellbeing, which is vulnerable to changes in rainfall variability potentially leading to enhanced flooding or drought. South Asia comprises a region of complex atmospheric dynamics and regional climate processes. Potential changes in these dynamics resulting from the warming induced by increasing greenhouse gas concentrations, combined with existing vulnerability to extreme weather events such as flooding due to low-lying topography, could put the region at severe risk from future climate changes (Caesar et al., 2015). The DECCMA project (Hill et al., this issue) aimed to assess the numerous potential impacts and adaptations to these climate changes on the populations of the Ganges-Brahmaputra-Meghna (GBM) and Mahanadi deltas. This paper describes how the climate information that underpins these assessments was generated.

The climate of South Asia is characterised by high temperatures, a monsoon season with heavy rainfall, periods of high humidity and strong seasonal variations. The dominant regional climate feature is the seasonal reversal of the large-scale atmospheric circulation between summer and winter months, resulting in the rainy season known as the ‘summer’ or ‘South Asian’ monsoon. The annual climate of South Asia can typically be separated into four distinct seasons: pre-monsoon (March-April-May, denoted as MAM), monsoon (June-July-August-September, denoted as JJAS), post-monsoon (October-November, denoted as ON), and winter (December-January-February, denoted as DJF). The summer monsoon season brings the highest accumulation of precipitation seen during the year, with around 70-80% of the region’s total annual precipitation falling within the JJAS season (Caesar et al., 2015; Kumar et al., 2013; Kumar et al., 2006).

Studies based on observational records have not revealed a significant trend in either increases or decreases in average monsoon rainfall across India as a whole, however regional trends across meteorological subdivisions of India and Bangladesh are apparent

(Rupa Kumar et al., 2002; Dash et al., 2007; Kumar et al., 2013). On daily timescales, some studies have observed an increase in the frequency of extreme rainfall days across much of the subcontinent, possibly due to increased moisture content and warmer sea surface temperatures in recent history (Christensen et al., 2013; Goswami et al., 2006). Although single extreme rainfall events such as the severe flooding event in July 2005 across Mumbai cannot be directly attributed to climate change (Kumar et al., 2013), many studies around the world are demonstrating how climate change is increasing the risk of such extreme events happening (e.g. Pall et al., 2011; Schaller et al., 2016; Philip et al., 2018).

A number of previous modelling studies, making use of both global climate model (GCM) and regional climate model (RCM) information for South Asia, have been performed to assess future impacts of climate change for this vulnerable region (Bhaskaran et al., 1996; Ueda et al., 2006; Kumar et al., 2006; Islam et al., 2008; Krishna Kumar et al., 2011; Sabade et al., 2011; Kumar et al., 2013; Bal et al., 2015; Caesar et al., 2015). There is a strong consensus amongst climate projection studies for increases in temperatures across much of South Asia by the end of the 21st century, with a spread in the magnitudes dependent on greenhouse gas emission scenario and employed methodology (Caesar et al., 2015; Kumar et al., 2013; Christensen et al., 2013; Kumar et al., 2006). Similarly, a number of studies project an increase in annual precipitation for South Asia, and particularly Bangladesh, with the intensity of heavy precipitation events projected to increase across the country (Caesar et al, 2015; Sabade et al., 2011; Ueda et al., 2006). Current climate model capabilities in the realism of their simulation of summer monsoon characteristics are varied. Previous modelling studies suggest both a potential increase and decrease in the associated strength of the summer monsoon circulation in the 21st century, highlighting the complexity of modelling the dominant climate processes within this region (Janes & Bush, 2012; Kripalani et al., 2007; Tanaka et al., 2005). To date, climate change studies focused on South Asia are somewhat limited, and many are based on results from a singular modelling experiment. One study (Kumar et al., 2013) takes a multi model approach to better explore climate variability and change in South Asian climate dynamics, rather than relying on output from a singular future climate scenario. Taking an ensemble approach (Kumar et al., 2013; Jacob et al., 2007; Reichler and Kim, 2008), whereby results from multiple modelling activities is considered for analysis, provides a range of plausible climate changes. These are then relevant to undertaking a comprehensive assessment of risks and responses to climate change which is not possible when results are drawn from single scenario of future climate.

This study aims to help address this knowledge gap, and describes the use of an ensemble of three RCM simulations to generate high-resolution climate datasets over South Asia for assessing climate impacts in the GBM and Mahanadi deltas. Realistic representation of precipitation during the summer monsoon is important for producing user-relevant projections of regional climate for use in downstream impacts models due to the dominance of this season in providing much of the regional's total annual precipitation. For this reason, the analysis within this paper focuses mainly on the summer monsoon season of JJAS.

Section 2 of the paper summarizes the use of climate models and the model selection process taken in this study to produce three RCM simulations. Section 3 validates results from these RCM simulations against both observational datasets and their respective driving GCMs. Sections 4 and 5 investigate potential changes in key climate characteristics under increasing greenhouse gas emissions, followed by a summary of discussions and conclusions based on the results outlined here.

2. MODEL SELECTION AND DOWNSCALING

2.1 DOWNSCALING GLOBAL CLIMATE MODELS

The most recent assessment report of the Intergovernmental Panel on Climate Change (IPCC) used ensembles of GCM simulations from the Coupled Model Intercomparison

Project phase 5 (CMIP5) (Taylor et al., 2012) to provide projections of future climate conditions for regions of the world, including South Asia (IPCC, 2013; IPCC, 2014). GCMs are an invaluable tool for assessing potential climate change resulting from increased greenhouse gas emissions, and are useful for assessing potential changes in large-scale global phenomena such as the summer monsoon over South Asia. While suitable as a basis for an overall narrative for future regional climate changes, these coarse-resolution simulations do not provide information at high enough resolution to guide detailed assessment of the impacts of climate change through the use of downstream impacts models (e.g. hydrological and agricultural models).

To overcome the limitations of the coarse resolution GCMs, which typically have grid cells hundreds of kilometres across, high-resolution physically-consistent datasets for a large range of relevant climate variables can be generated through ‘dynamical downscaling’, whereby GCM output is used to drive a high-resolution RCM. RCMs are better able to represent local topography, coastlines, land use and regional atmospheric processes than coarse-resolution GCMs. They can add significant detail to the information obtained from GCMs, in particular for regional climate impacts studies and analyses of extreme events (Bal et al., 2015; Caesar et al., 2015; Kumar et al., 2013; Krishna Kumar et al., 2011).

2.2 SELECTION OF GCMS FOR DOWNSCALING

The CMIP5 GCMs provide simulations of the future climate forced with different scenarios for “radiative forcing”, or the energy imbalance of the climate system due changing greenhouse gas and aerosol concentrations in the atmosphere. These scenarios are known as Representative Concentration Pathways (RCPs) (Moss et al., 2010; van Vuuren et al., 2014). The CMIP5 dataset includes simulations of four different RCPs using over 40 GCMs (although simulations are not available for every RCP/GCM combination) and is considered to provide reasonable sampling of uncertainties in future climate conditions on large spatial scales. Ideally, we would consider a large number of climate datasets to fully sample uncertainties in future climate changes and resulting impacts. However, limited resources for running both RCM simulations and downstream impact model simulations meant that this was impractical. Therefore, a single RCP scenario (RCP 8.5) was selected for consideration in the DECCMA project (Kebede et al., 2018). This allowed us to focus on sampling the range of uncertainty arising from the use of different climate models. RCP 8.5 is a scenario depicting the highest greenhouse gas emissions, assuming high energy demand due to large population increases and slow rates of development and adaptation (Riahi et al., 2011). It is therefore expected to give a strong, discernible climate change signal in modelling results. Given that climate and impacts modelling constraints restricted us to running only three downscaled simulations, we focused on sampling uncertainty in the GCMs as the main source of modelling uncertainty at regional scales (Deque et al. 2005, Kendon et al., 2010) and thus used a single RCM (HadRM3P) for the downscaling activities performed here. HadRM3P has been tested and verified for accurate performance for a variety of regions around the world (Mearns et al., 2013; James et al., 2014; Massey et al., 2014; Bal et al., 2015; Centella-Artola et al., 2015; Williams et al., 2015).

In selecting CMIP5 models for downscaling with HadRM3P we followed the approach of McSweeney et al. (2015) and built on its application in a recent collaborative project with the Met Service Singapore (see Table 1, Marzin et al., 2015). This approach advises selecting GCMs for downscaling based on two criteria:

1. All selected GCMs should have a satisfactory simulation of relevant aspects of the recent climate of the region of interest.

2. Future climate changes in the region of interest simulated by the ensemble of selected GCMs should span the range of future climate changes spanned by the full ensemble of satisfactory GCMs.

HadGEM2-ES	Met Office Hadley Centre
ACCESS1-0	Commonwealth Scientific and Industrial Research Organization and Bureau of Meteorology
BCC-CSM-1-1-M	Beijing Climate Center
CanESM2	Canadian Centre for Climate Modelling and Analysis
CMCC-CM	Centro Euro-Mediterraneo per I Cambiamenti Climatici
CNRM-CM5	Centre National de Recherches Meteorologiques
CSIRO-Mk3-6-0	Commonwealth Scientific and Industrial Research Organisation in collaboration with the Queensland Climate Change Centre of Excellence
GFDL-CM3	Geophysical Fluid Dynamics Laboratory
GFDL-ESM2G	Geophysical Fluid Dynamics Laboratory
IPSL-CM5A-LR	Institut Pierre-Simon Laplace

Table 1. Model names and institution details for the 10 CMIP5 GCMs considered for downscaling in this study.

In addressing the first criterion, a number of models were immediately eliminated from the selection due to either a) a lack of robust monsoon dynamics as described in McSweeney et al. (2015), or b) incorrect climate characteristics or responses identified in a previous project (Marzin et al., 2015). No additional GCM assessments specific to the South Asia region was performed as these were part of the work undertaken by McSweeney et al. (2015) and the Met Service Singapore project, and so applicable to our region of interest.

To address the second criterion, we examined climate changes between the 1961-1990 time period and the 2070-2099 time period in the RCP 8.5 simulations of the different CMIP5 GCMs. Future changes in annual and seasonal mean temperature and precipitation were calculated over a region covering the Mahanadi and GBM basins (15-30˚N, 80-95˚E). These results were subsequently used to select GCMs that spanned as much as possible of the range of future climate changes simulated by the full CMIP5 ensemble, for both the annual and seasonal timescales (Fig 1). Through assessing the spread of models on both annual and seasonal timescales, we were able to identify three models which sufficiently span the range of plausible future changes within the full set of GCMs available for downscaling. We then cross-referenced these GCMs with the findings of McSweeney et al. (2015), to ensure adequate performance over larger monsoon regions. The three GCMs chosen for downscaling within the DECCMA project were HadGEM2-ES, CNRM-CM5, and GFDL-CM3. Each of these global models has slightly different grid resolutions: 1.25° latitude X 1.875° longitude for HadGEM2-ES, 1.4° latitude X 1.4° longitude for CNRM-CM5, and 2.0° latitude X 2.5° longitude for GFDL-CM3.

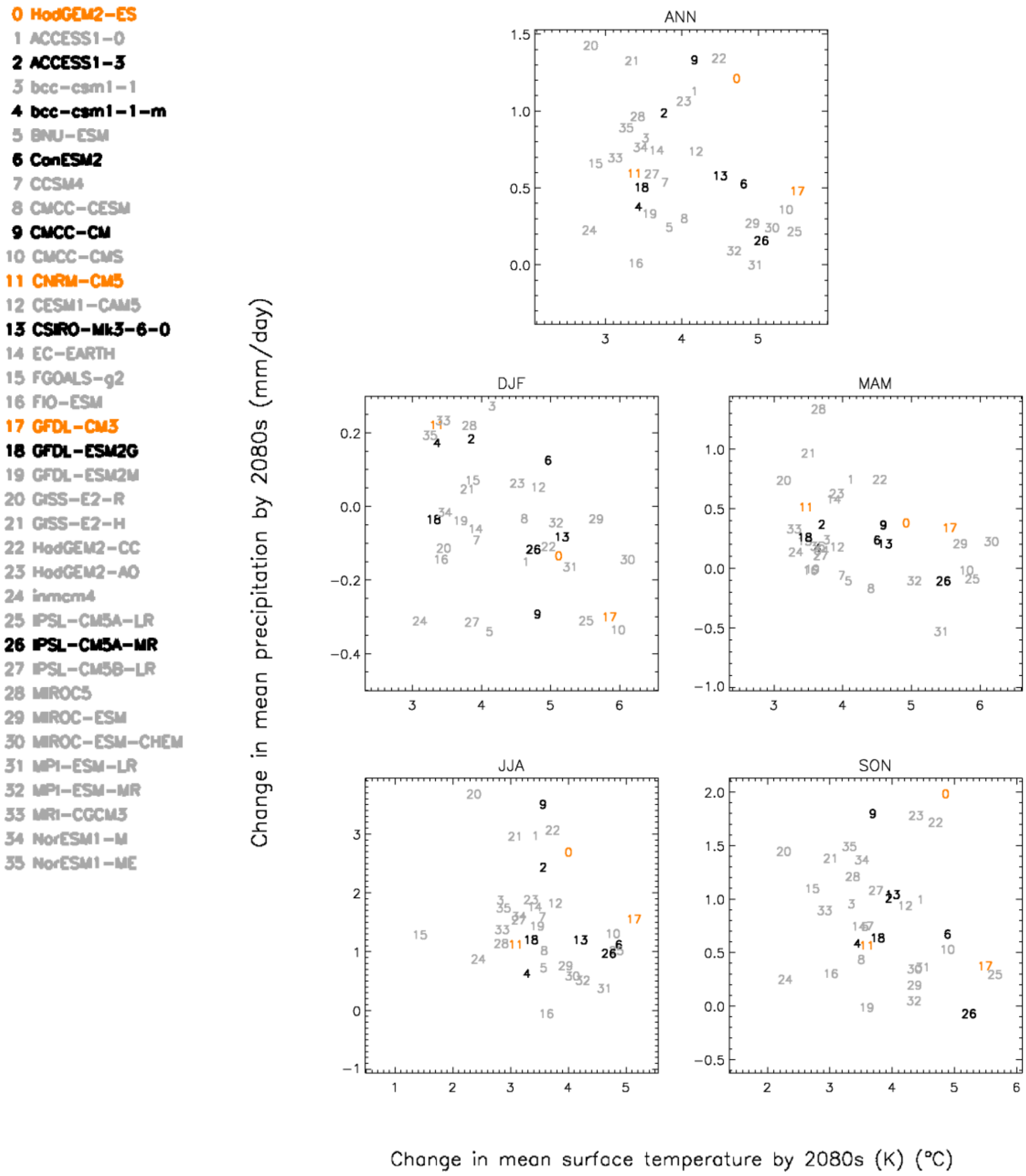

Figure 1: CMIP5-simulated future climate changes for RCP 8.5 for a region covering the Mahanadi and GBM basins (15-30˚N, 80-95˚E). Changes in annual mean temperature and precipitation between 1961-1990 and the 2080s are shown in the top panel. Subsequent panels show the same analysis for seasonal means (DJF = December, January, February; MAM = March, April, May; JJA = June, July, August; SON = September, October, November). Grey numbers represent GCMs that could not be downscaled due to a lack of output suitable for input to an RCM. Orange numbers indicate the three GCMs that were selected for downscaling in the DECCMA project.

Seasons outside of the monsoon season may be of interest to those assessing climate change impacts and are important to the regional climate dynamics of the region. Note, however, that it was not possible to sample the full range of changes in annual and seasonal mean temperature and precipitation with just these three GCMs selected. Most obviously, the selected GCMs do not span much of the uncertainty in CMIP5-simulated future changes in seasonal mean precipitation for the March, April, May (MAM) season (Fig 1). In this season, all three selected GCMs simulate future increases in seasonal mean precipitation of 0.5mm/day or less. However, some CMIP5 GCMs simulate future decreases in seasonal mean precipitation for this season and some simulate increases of greater than 0.5mm/day. Thus, one consequence of the limited number of GCMs used in this study is to exclude those simulating the most extreme future climate changes.

2.3 REGIONAL CLIMATE MODELS

Coarse resolution output from three different GCMs selected above was used as lateral boundary and sea-surface conditions to drive the Met Office Hadley Centre RCM, HadRM3P (Jones et al., 2004; Massey et al., 2014). This is a high-resolution limited area model, which underlies the Providing Regional Climates for Impacts Studies (PRECIS) regional modelling system. The RCM simulations undertaken here using HadRM3P are at a resolution of 0.22° X 0.22° (approximately 25 km), with 19 vertical levels and 4 soil levels. The chosen model domain covers South Asia, allowing for the development of full mesoscale circulation patterns that influence the monsoon system (Fig 2). A considerable amount of research has been done to assess the appropriate domain choice for capturing monsoon dynamics over India (Bhaskaran et al., 2012). In addition, the choice of this domain will allow the information produced within the DECCMA project to be applicable to a number of current and future research and collaboration opportunities in the region.

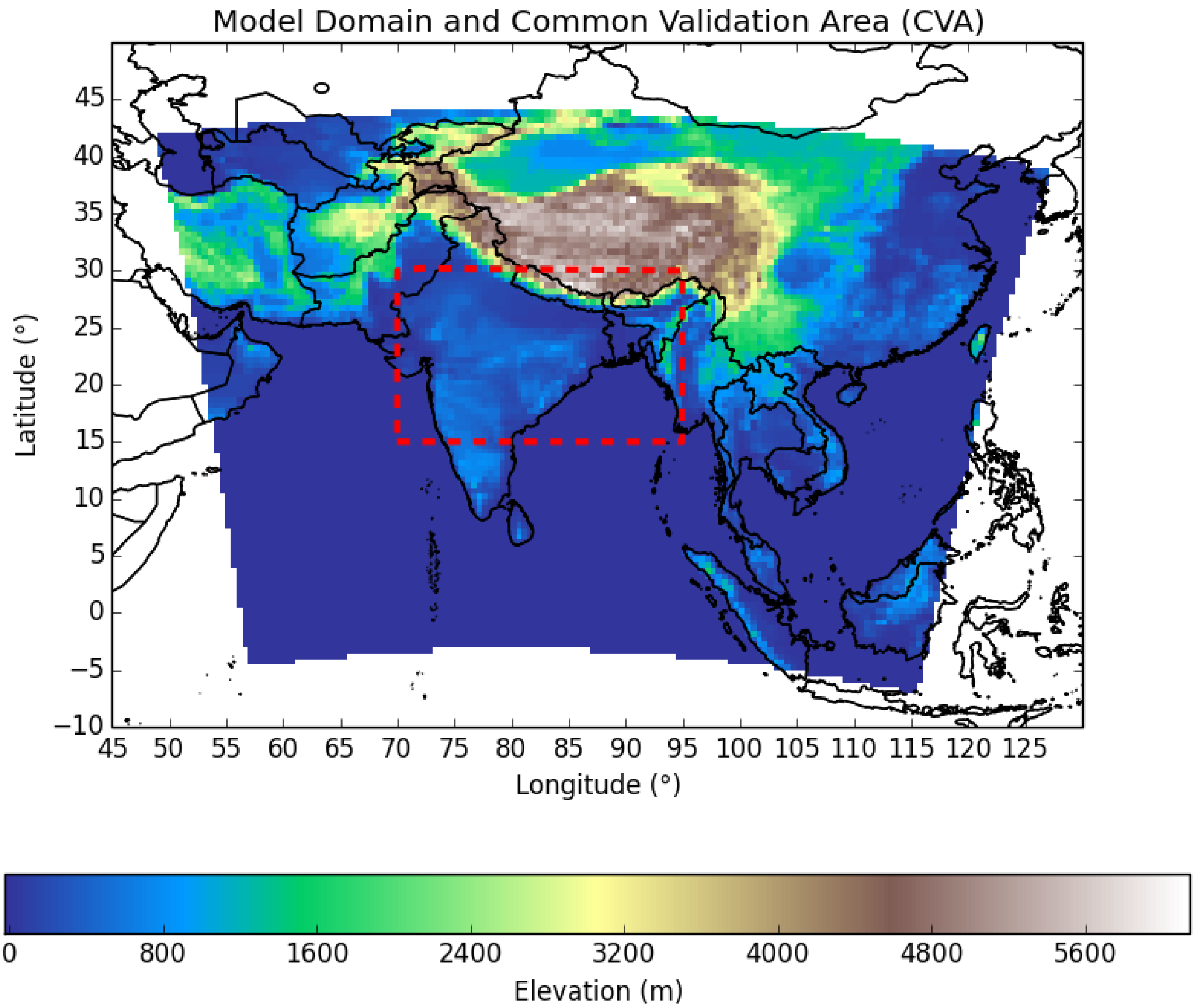

Figure 2: Downscaling domain for South Asia, depicting the model elevation (m). Red dashed box indicated the common validation area (CVA) used for comparison of annual cycles in RCMs and observed temperature and precipitation. The CVA contains the following latitude and longitude ranges: 15-30° N, 70-95° E.

3. VALIDATION OF RCM SIMULATIONS

RCM simulations were validated against climate observations following methods by Caesar et al. (2015). Model outputs were compared to fine-resolution gridded temperature, precipitation, and lower level wind observations and reanalyses (a full list of datasets used in this study can be found in Table 2). Note that other gridded observational temperature and precipitation datasets are available, but not all of these are suitable for validating RCM simulations. For example, the GPCP and CMAP precipitation datasets (Adler et al., 2003;

Xie and Arkin, 1997) have a much coarser spatial resolution (2.5° x 2.5°) than the RCM simulations.

Dataset	Abbrev.	Variables	Resolution	Period	Reference
Climatic Research Unit TS3.10	CRU	Temperature, Precipitation	0.5° x 0.5°	1901-2009	Harris et al. (2014)
University of Delaware	UDEL	Precipitation	0.5° x 0.5°	1950-1999	Willmott & Matsuura (1995)
APHRODITE version 1003R1 dataset (Aph.v10)	APHRODITE	Precipitation	0.25° x 0.25°	1951-2007	Yatagai et al. (2012)
Global Precipitation Climatology Centre	GPCC	Precipitation	0.5° x 0.5°	1901-present	Schneider et al. (2015)
Global Historical Climatology Network – Climate Anomaly Monitoring System	GHCN-CAMS	Temperature	0.5° x 0.5°	1948-present	Fan and van den Dool (2008)
ERA-Interim	ERAI	Winds	0.75° x 0.75°	1979-present	Dee et al. (2011)

Table 2: Gridded observational temperature and precipitation datasets used for RCM simulation validation.

In this study, climatological mean surface air temperature and precipitation data averaged over the 1971-2000 (30-year) period from the RCM simulations were compared with observed datasets averaged over the same time period. For the comparison of lower-level winds (crucial to ensuring the realistic simulation of monsoon dynamics), climatological mean data for the 1979-2000 (22-year) period was used due to limited timescales available within the ERAInterim dataset. To promote a fair comparison, all data were regridded to the coarsest of the spatial resolution of the datasets (i.e. regridded onto a 0.5° x 0.5° grid for temperature and precipitation, and 0.75° x 0.75° for lower-level winds). Sea grid cells in the RCM data were masked out to be consistent with the observational temperature and precipitation datasets, which have no data over oceanic points.

The RCM and observational data were then compared in two ways. Firstly, annual cycles based on monthly mean data averaged over a common validation region (CVA) shown in Figure 2 were calculated. This region covers much of the GBM river basin and the entire Mahanadi river basin, both foci of the DECCMA project. However, it also extends further south to include the area of maximum monsoon precipitation from the summer monsoon, allowing for the assessment of typical monsoon characteristics. Secondly, maps of climatological mean data for June-September (JJAS) season were compared, as this season is the dominant provider of the region’s total annual precipitation. For brevity, only one observational dataset was used in each of these spatially-explicit comparisons: CRU for temperature, GPCC for precipitation, and ERA-Interim for winds.

Additionally, the RCM data were compared against corresponding data from their respective forcing GCM simulations, both averaged over the 1971-2000 time period. As with observational data, the RCM data were regridded to the coarser resolution of the GCM data and then compared using maps of the June-September (JJAS) season. This methodology helps us to verify that, on larger spatial scales, the RCM simulations are consistent with their forcing GCM simulations.

3.1 Temperature

Figure 3 compares the 1971-2000 climatological mean annual cycles in surface air temperature for the CVA region, for each of the three RCM simulations as well as the CRU and GHCN-CAMS observational datasets. The CRU dataset is marginally warmer than the GHCN-CAMS dataset, particularly during the monsoon season. These differences could be down to the number of stations used in the gridding process, interpolation methods invoked, or in the application of any elevation corrections.

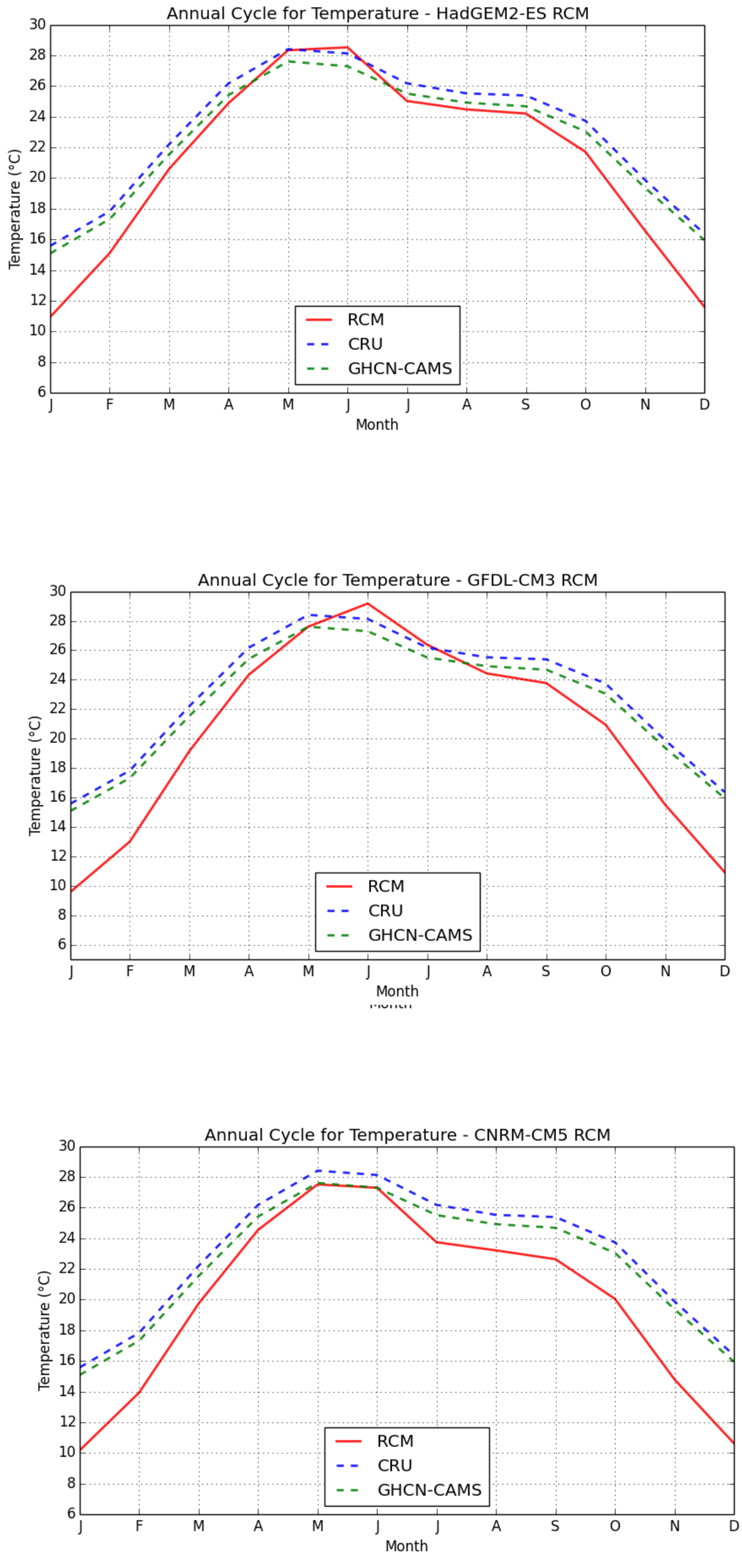

Figure 3: 1971-2000 climatological mean annual cycles in surface air temperature for each of the three RCM simulations and the CRU and GHCN-CAMS observational datasets.

All three models are able to simulate fluctuating temperatures across an annual cycle, with varying amplitudes across the ensemble (Fig 3). During the months of April-September, the HadGEM2-ES-forced simulation and the GFDL-CM3-forced simulation are both able to realistically capture summer temperature patterns. The CNRM-CM5-forced simulation has an additional slight cold bias of approximately 1°C in these summer months. All three models show a pronounced cold bias during the winter months, ranging from approximately 3-4°C for the HadGEM2-ES-forced simulation to 5-6°C for the GFDL-CM3-forced simulation.

To better characterise the nature of the cold biases in temperature described above, spatial comparisons between the three models and the CRU observational dataset are shown in Figure 4. In the monsoon season (JJAS), all three RCM simulations depict a small cold bias for most of the region, with maximum biases occurring over the Himalayas (Fig 4). Over central India and Bangladesh, both the HadGEM2-ES-forced simulation and the CNRM-CM5-forced simulation show slight cold bias, whereas temperature biases in the GFDL-CM3-forced simulation are minimal for this region. Across the whole domain, it is clear that the cold biases in the CNRM-CM5-forced simulation are generally larger than in the other two simulations (consistent with Fig 3.), with no warm biases anywhere in the region. It is possible that in this topographically complex region, differences in elevation between the RCM and the observing sites contributing data to the observational dataset are leading to this apparent bias, which is more pronounced during the winter months (Fig 3). In mountainous regions, observational stations are often located at lower elevations within accessible valleys, which can lead to warm biases within gridded observational datasets as conditions at higher elevations are not accurately captured. This results in an apparent cold bias within RCM simulations, particularly in the winter months, and has been found in a number of previous studies using a range of RCMs over South Asia (Rupa Kumar et al., 2006; Islam et al., 2009; Gu et al., 2012). For the purpose of this validation, which focuses solely on the monsoon season of JJAS, no correction for height differences between model results and observational datasets has been applied.

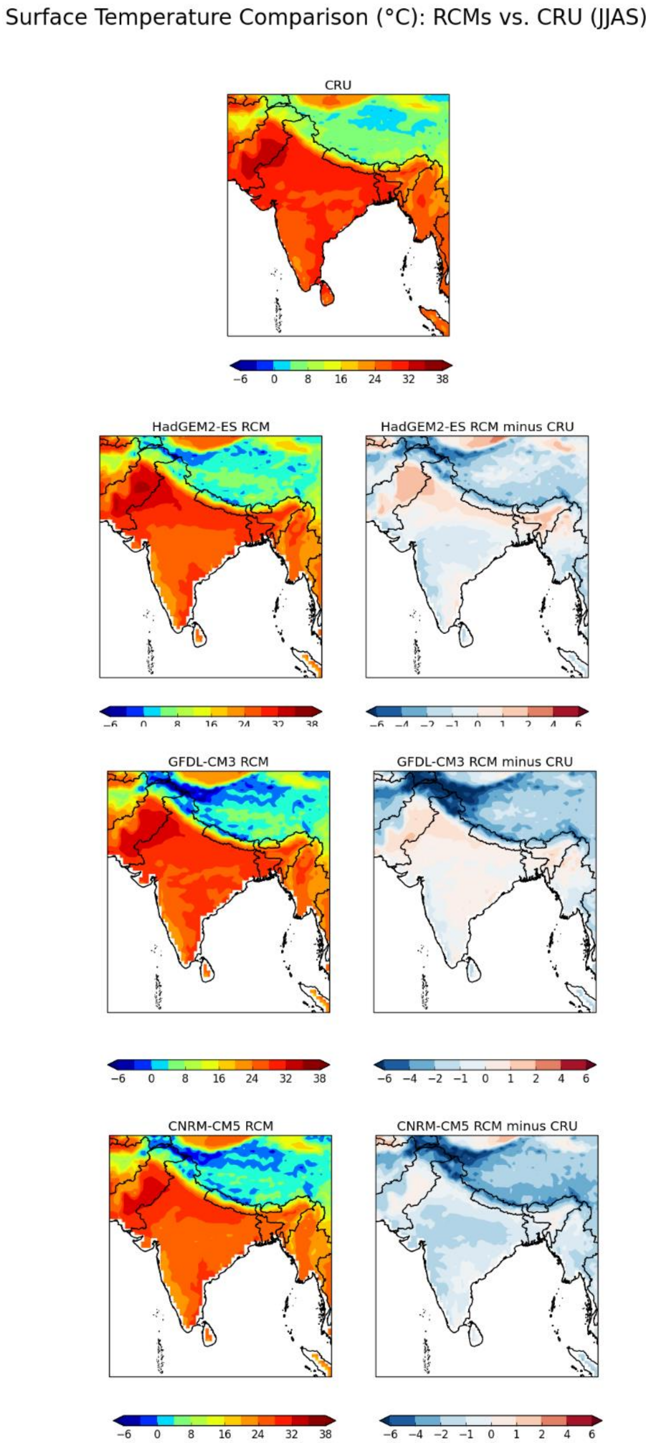

Figure 4: 1971-2000 climatological mean surface air temperature for JJAS for each of the RCM simulations and the CRU observational dataset. Differences between the RCM and CRU datasets are also shown.

When comparing the driving GCM data to observations, large cold biases over the Himalayas are also present, but to a lesser extent for the HadGEM2-ES GCM than for the other two GCMs (not shown). RCM biases over the rest of the region do not appear to be directly inherited from their forcing GCMs, and are therefore likely to be a product of the RCM itself. However, a component of the biases between the RCM simulations and the gridded observational datasets may be due to the formulation of the observational datasets, which in themselves are inherently uncertain over regions of complex topography.

Comparing regridded RCM output to results from the driving GCM (Fig 5) suggests that both the HadGEM2-ES-forced RCM simulation and the CNRM-CM5-forced simulation are slightly colder in most of the region, including in the ocean, than their respective driving GCMs. This difference in temperature is largest in the Himalayas, which could again be related to differences in topography across the RCM and GCM implementation. A region of warmer temperatures extends eastwards from Pakistan across northern India and Bangladesh, consistent with the comparison of HadGEM2-ES-forced RCM results with observations. Conversely, the GFDL-CM3-forced RCM simulation has a small region of warmer temperatures compared to its forcing GCM, even extending into the Himalayas. These results suggest general large-scale RCM-GCM consistency, but further confirms that biases in the RCM results shown here are not entirely inherited from their driving GCMs.

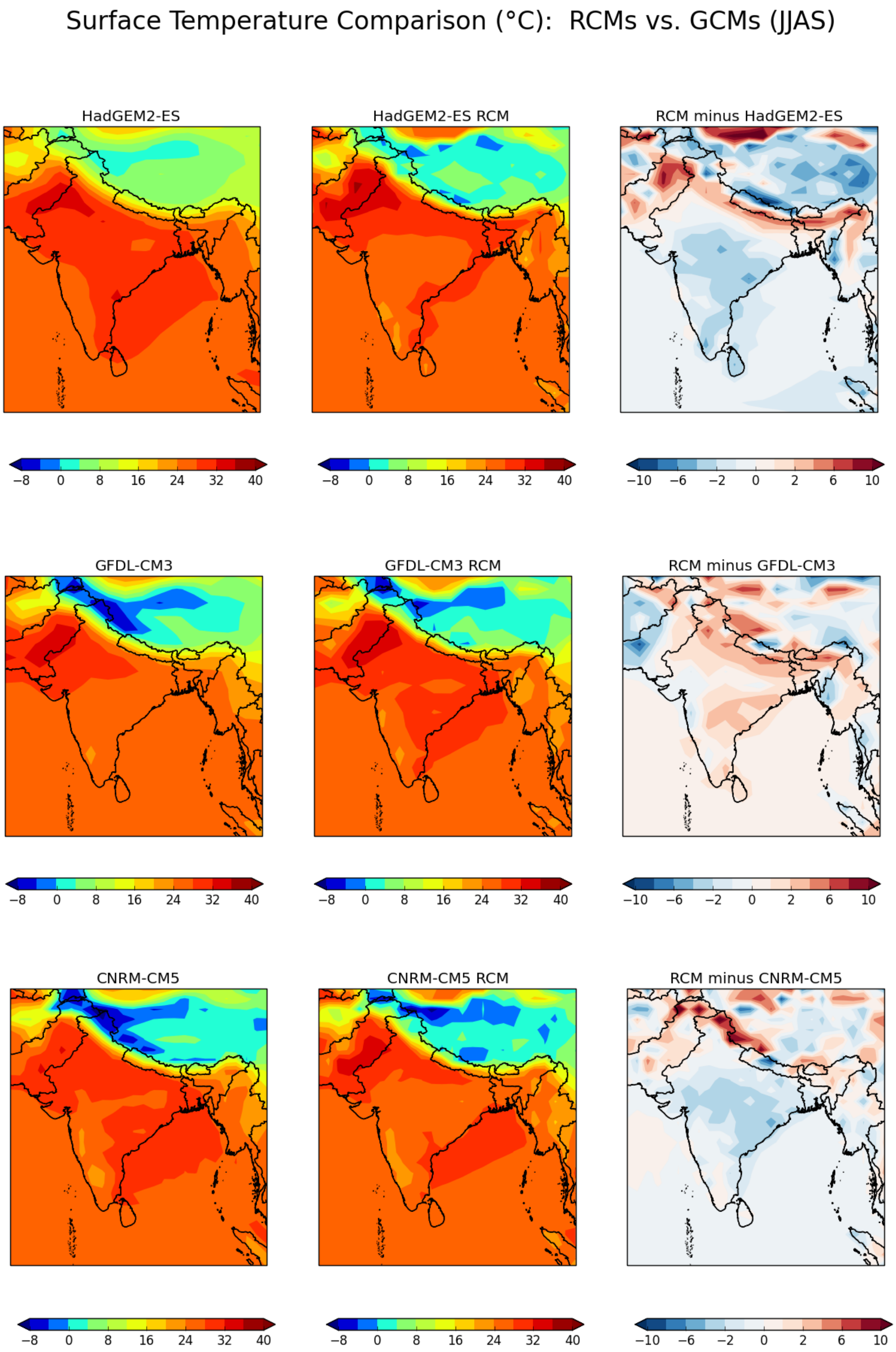

Figure 5: 1971-2000 climatological mean surface air temperature for JJAS for each of the RCM simulations and for their corresponding forcing GCM. Differences between the RCM and GCM datasets are also shown.

3.2 Precipitation

Figure 6 compares the 1971-2000 climatological mean annual cycles in precipitation averaged over the CVA region depicted in Figure 2, for each of the three RCM simulations and the CRU, UDEL, GPCC and APHRODITE observational datasets. All four observational datasets show a distinct winter dry season followed by increasing precipitation through the onset of the summer monsoon in May with the wettest months in July and August, followed by a decline in precipitation in October and November. The absolute amount of precipitation differs between the observational datasets, especially during the wetter months, which illuminates the high level of uncertainty across observational datasets in this region and the difficulty in using gridded observational datasets to validate RCM information. In these months, the GPCC dataset consistently shows the greatest precipitation and the APHRODITE dataset consistently shows the least precipitation. Such differences between observational datasets have been found in other studies (Prakash et al., 2014; Herold et al., 2016), and can arise through different networks of observing stations being used and different methods of interpolating data from the stations onto a spatial grid.

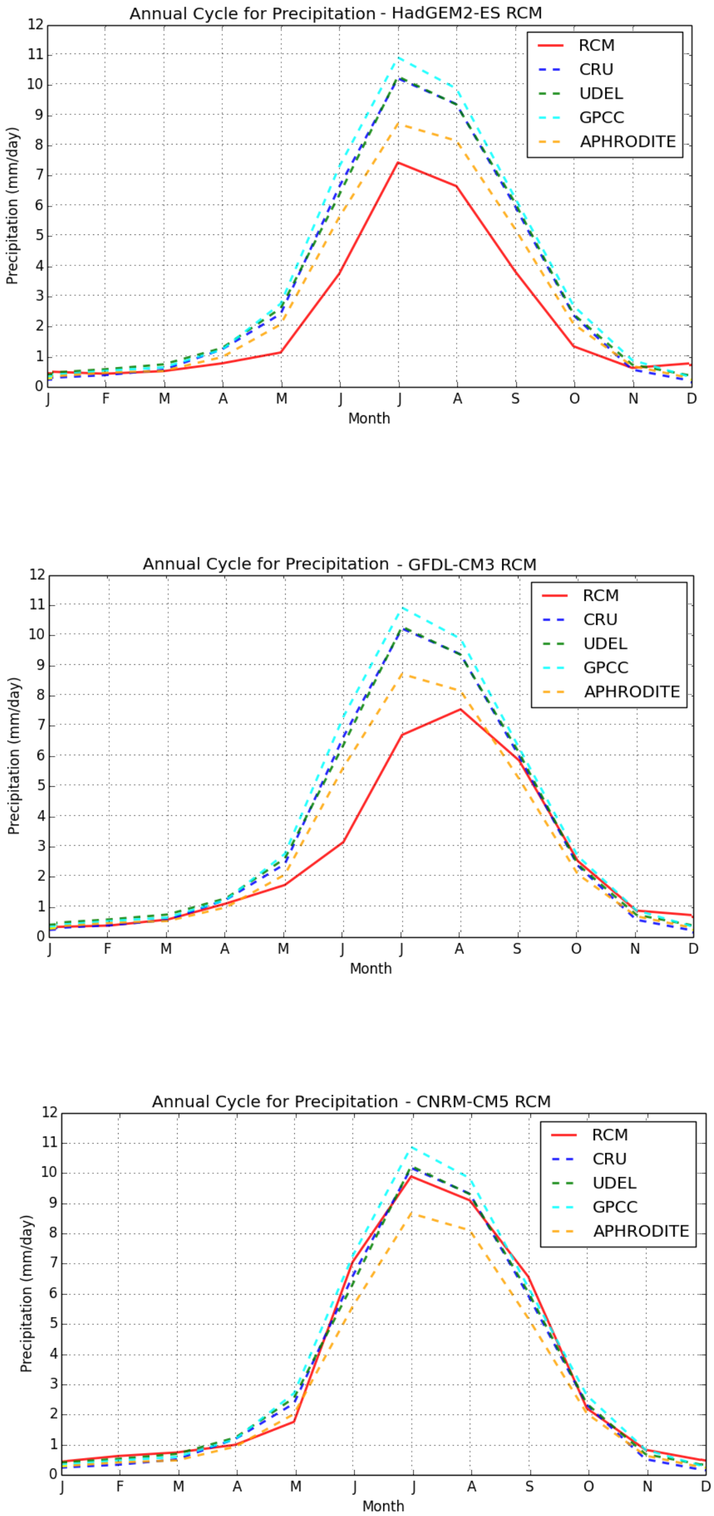

Figure 6: 1971-2000 climatological mean annual cycles in precipitation (mm/day) for each of the three RCM simulations and the CRU, UDEL, GPCC, and APHRODITE observational datasets.

The HadGEM2-ES-forced RCM simulation reproduces the annual cycle in regionally-averaged precipitation, but has a significant dry bias relative to all of the observational datasets throughout the summer monsoon season. Likewise, the GFDL-CM3-forced simulation has an overall dry bias in CVA-average precipitation relative to all four observational datasets. However, the maximum monthly mean precipitation is later in the GFDL-CM3-forced simulation than in the observations, occurring in August rather than in July. The simulated monthly mean CVA-average precipitation values match the observations well in September and October. It is possible that there is a dry bias in the simulation during the build up to the monsoon and the monsoon itself, but not during the monsoon decay. Alternatively, the monsoon rains could be delayed in the simulation relative to the observations. A comparison of the simulated and observed monsoon circulation and associated onset and cessation would be necessary to test these hypotheses. Unfortunately, fell outside the scope of the DECCMA project, but is currently being investigated in follow-on work.

As in the HadGEM2-ES-forced and GFDL-CM3 forced simulations, the CNRM-CM5-forced simulation reproduces the annual cycle in CVA-average precipitation. However, in contrast to the other two models, the simulated precipitation in the monsoon season lies within the observational uncertainty described by the four observational datasets.

In spatial maps of climatological monsoon precipitation (Fig 7), the regional extent of precipitation biases is similar across all three models, with a few regions of noteworthy differences. The HadGEM2-ES forced simulation depicts dry biases of more than 2mm/day extending across much of India and Bangladesh. The areas of dry biases correlate well with areas of warm biases in Figure 4, suggesting the latter result from reduced evaporative cooling and/or enhanced solar radiation respective from lower precipitation and associated cloud clover. Dry biases in the HadGEM2-ES simulation are partially offset by wet biases in the Himalayas. The spatial patterns of precipitation biases in the GFDL-CM3-forced depict a slightly larger extent of dry biases over India, particularly in the Mahanadi basin region. Dry precipitation biases in the CNRM-CM5-forced simulation are much less extensive than the other two models, which contributes to the better match between the simulated and observed regionally-average precipitation values for the CNRM-CM5-forced simulation (Fig 6). Overall, all three models have lesser spatial biases compared to observations than their respective forcing GCMs (not shown).

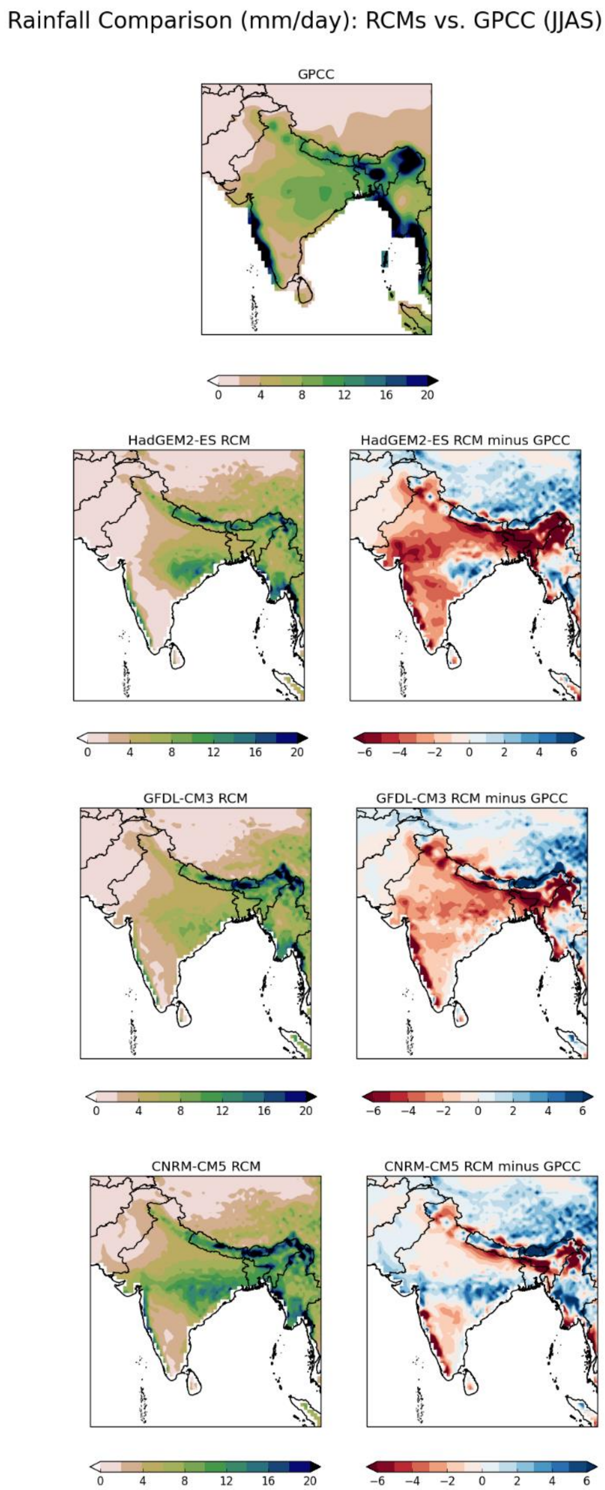

Figure 7: 1971-2000 climatological mean precipitation for JJAS for each of the RCM simulations and the GPCC observational dataset. Differences between the RCM and GPCC datasets are also shown.

When comparing to results from the driving GCMs (Fig 8), the HadGEM2-ES-forced RCM simulation has two notable anomalies relative to the original HadGEM2-ES GCM: a large dry region in northeast India extending across Bangladesh and a strong wet anomaly in central India (bringing it closer to observations) and over the Bay of Bengal. The GFDL-CM3-forced RCM simulation also has a wet anomaly over the Bay of Bengal relative to its original GCM, but contains a much more widespread dry anomaly over most of India and into parts of the Himalayas, Tibetan Plateau and off the southeast coast into Sri Lanka. The CNRM-CM5 forced RCM simulation is wetter than the driving GCM across most of the region including in central India and Bangladesh (again bringing it closer to observations) with the largest differences in the Bay of Bengal and the Arabian Sea. There is also a large dry anomaly off the east coast of Sri Lanka. All three RCMs are depicting enhanced precipitation over the Bay of Bengal with respect to their driving GCMs, which could be due to the finer model resolution and increased capability in capturing precipitation over complex topography.

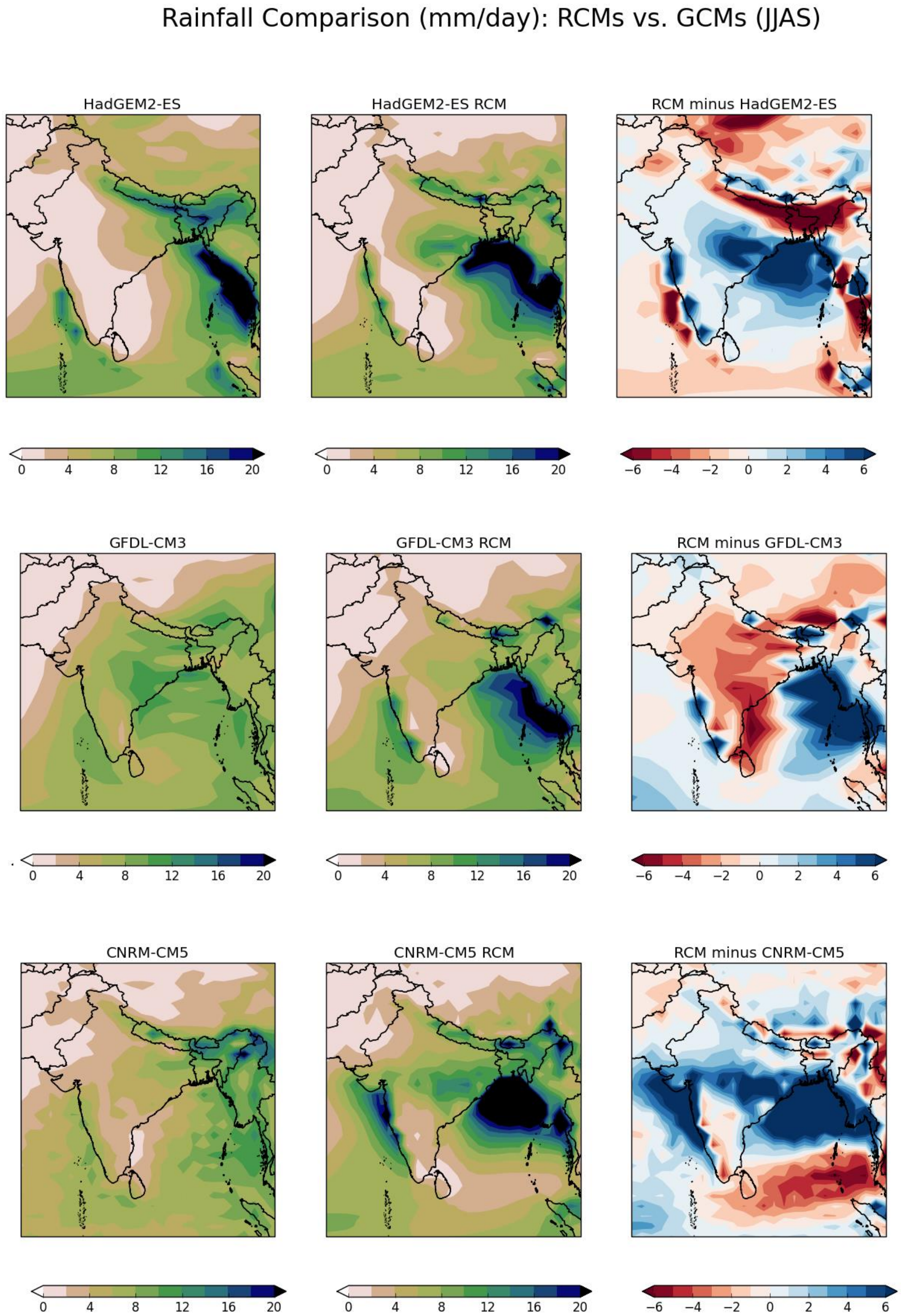

Figure 8: 1971-2000 climatological mean precipitation for JJAS for each of the RCM simulations and for their corresponding forcing GCM. Differences between the RCM and GCM datasets are also shown.

3.3 Lower-Level Winds (850hPa)

Figure 9 shows the spatial pattern in biases in lower-level (850 hPa) winds between each of the three RCM simulations and the ERA-Interim gridded dataset during the monsoon season, averaged over 1979 to 2000. The RCMs reproduce the monsoon circulation well, with the characteristic strong, moisture-laden westerly winds coming in from over the Arabian Sea present in all three simulations. The HadGEM2-ES-forced simulation has a positive bias of 4-6 m/s for westerly winds over Central India and extending eastward into the Bay of Bengal, Myanmar and Thailand. The GFDL-CM3-forced simulation has little to no spatial bias for lower-level winds, the most notable being a small positive bias over the Bay of the Bengal. The CNRM-CM5-forced simulation has a positive bias over central India and the Bay of Bengal. However, unlike the other two simulations, it has a negative bias of around 4 m/s off the south coast of India over Sri Lanka and the Indian Ocean. Biases in lower-level wind strength, particularly over central India, could help to explain the wet biases seen in these regions for two of the three RCM models (HadGEM2-ES-forced and CNRM-CM5-forced, see Fig 7), as stronger monsoon circulation could lead to increased convergence and associated monsoon precipitation over land.

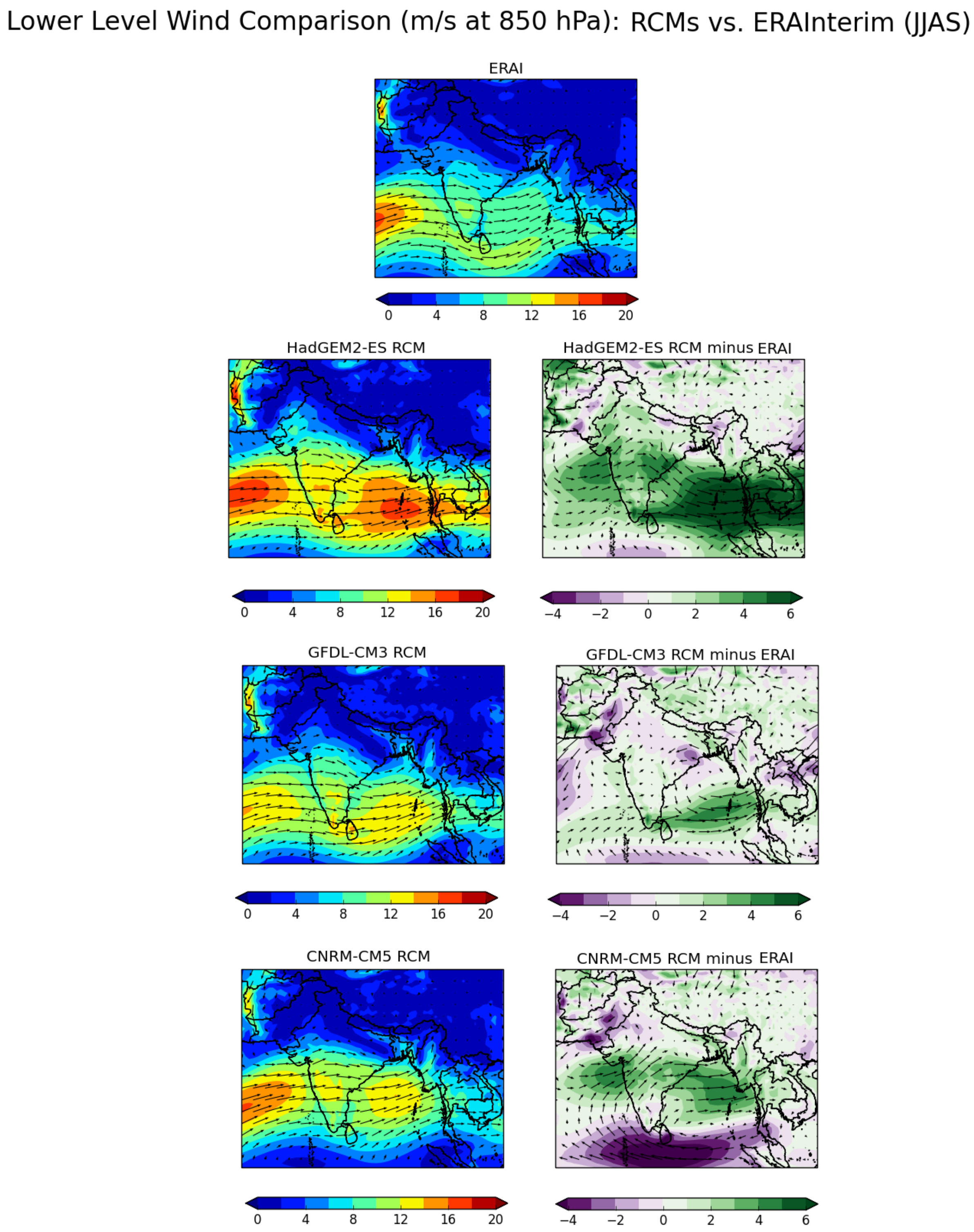

Figure 9: 1979-2000 climatological mean lower-level wind speeds (m/s) for JJAS for each of the RCM simulations and the ERA-Interim observational dataset. Differences between the RCM and ERA-Interim datasets are also shown.

To assess consistency with their driving GCMs, Figure 10 shows the spatial pattern in differences in lower-level winds between each of the three RCM simulations and their original forcing GCMs for the monsoon season, averaged over 1971 to 2000. White grid points on the spatial maps in Fig 10, predominantly located in the Himalayas, represent grid points for which the 850hPa pressure level intersects with the model topography, and were therefore omitted from subsequent analysis. The HadGEM2-ES-forced and GFDL-CM3-forced RCM simulations have minimal differences compared to the original GCM. The CNRM-CM5-forced RCM has more significant differences compared to its original GCM than seen in the other two RCMs, including a positive anomaly of around 4-6m/s starting over the Arabian sea and extending eastwards over India and into the Bay of Bengal. It also has a negative anomaly of around 4m/s off the south coast of India, across Sri Lanka and extending into the southern Bay of Bengal. This analysis indicates that the RCMs have large-scale consistency with their driving GCMs, particularly in the simulation of monsoon atmospheric dynamics.

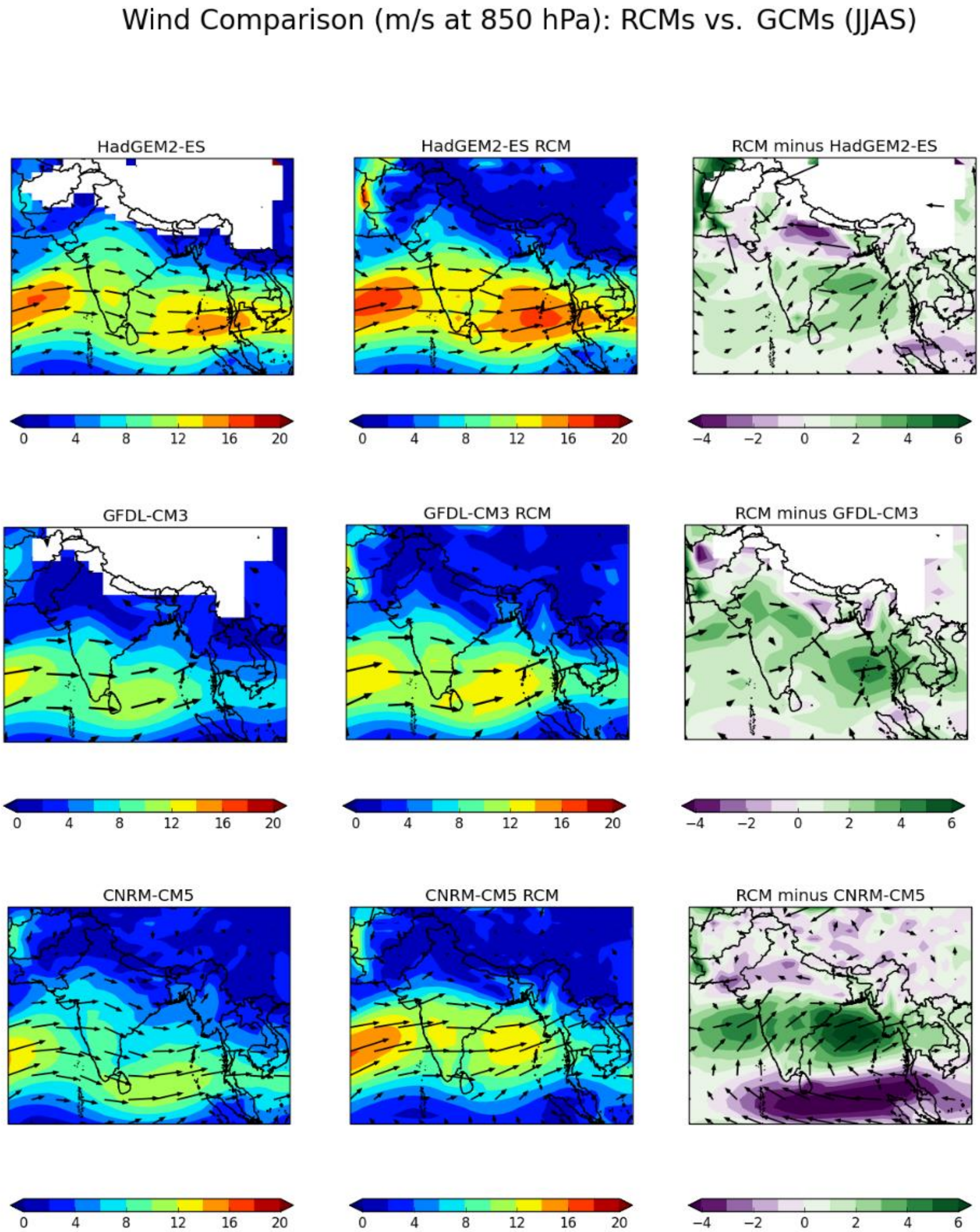

Figure 10: 1971-2000 climatological mean lower-level winds (m/s) for JJAS for each of the RCM simulations and for their corresponding forcing GCM. Differences between the RCM and GCM datasets are also shown

In summary, the validation undertaken in Section 3 confirms that the regional climate information produced by the three RCMs in this study, particularly focused on the monsoon season of JJAS, are reasonably aligned with observational datasets in their magnitude and spatial depiction of key characteristics inherent in the climate of South Asia. They are therefore ‘fit for purpose’, and suitable for use in downstream impacts modelling and adaptation work, both within the DECCMA project and more broadly in future impacts assessments for South Asia. A summary of key biases within the RCM simulations can be found in Table 3. While there are biases in RCM output with respect to observations, these biases are an expected occurrence when implementing RCMs over this complex region of interest, and do not affect the integrity of the information produced.

Simulation	Temperature	Precipitation
RCM forced by HadGEM2-ES	Timing of warm and cool seasons similar to observations. Overall cold bias for the region throughout the year, except in May-Jun, largest in winter (~4°C in Jan mean temperature). Cold biases across the entire region in winter. Much smaller local cold biases during summer, with warm biases in some parts of northern India and Bangladesh. Large cold bias in Himalayas throughout the year. More extreme variation in temperature between winter and summer than in observations.	Timing of wet and dry seasons similar to observations. Overall dry bias for the region during wet months. Large local dry biases in Bangladesh and eastern India throughout Mar-Nov, with dry biases across most of the region in Jun-Sep. Wet bias in Himalayas throughout the year and to the west of the Mahanadi Delta in Jun-Sep.
RCM forced by CNRM-CM5	Timing of warm and cool seasons similar to observations. Overall cold bias for the region throughout the year, larger in winter than in summer (~1°C in monthly mean temperature in May-Jun, ~5°C in Jan mean temperature). Cold biases across the entire region throughout the year, except Mar-May, in which there are warm biases in Bangladesh and eastern India. Large cold bias in Himalayas throughout the year. More extreme variation in temperature between winter and summer than in observations.	Timing of wet and dry seasons similar to observations. Little overall bias for the region throughout the year. Large local dry biases in Bangladesh and eastern India in Mar-May, with more extensive dry biases in Jun-Sep. Wet bias in Himalayas throughout the year and across central India in Jun-Sep.
RCM forced by GFDL-CM3	Timing of warm and cool seasons similar to observations. Overall cold bias for the region throughout the year, except in Jun, largest in winter (~6°C in Jan mean temperature).	Maximum monthly precipitation later in the year than in observations. Overall dry bias for the region during May-Aug.

	Cold biases across the entire region in winter. Very small biases across most of the region during summer. Large cold bias in Himalayas throughout the year. Much more extreme variation in temperature between winter and summer than in observations.	Large local dry biases in Bangladesh and eastern India in Mar-May, with dry biases across most of the region in Jun-Sep. Wet bias in Himalayas throughout the year.

Table 3: Summary of comparisons of RCM simulations with temperature and precipitation observations, focused on the GCM basin and northern India.

4. CLIMATE PROJECTIONS

To assess potential changes in future climate over South Asia, differences between a future time period (2070-2099) and a historical baseline period (1971-2000) were compared for key climate variables. Projected changes were calculated with respect to a particular model's own present day climate, thereby reducing the influence of biases in the analysis, as it is assumed these model biases would still be present in the future time period.

4.1 Temperature

Figure 11 compares the simulated 2070-2099 climatological mean surface air temperatures under the RCP 8.5 scenario to the simulated mean surface air temperature for 1971-2000, for each of the three RCM simulations during the monsoon season. All three RCM simulations project strong increases in surface temperatures.

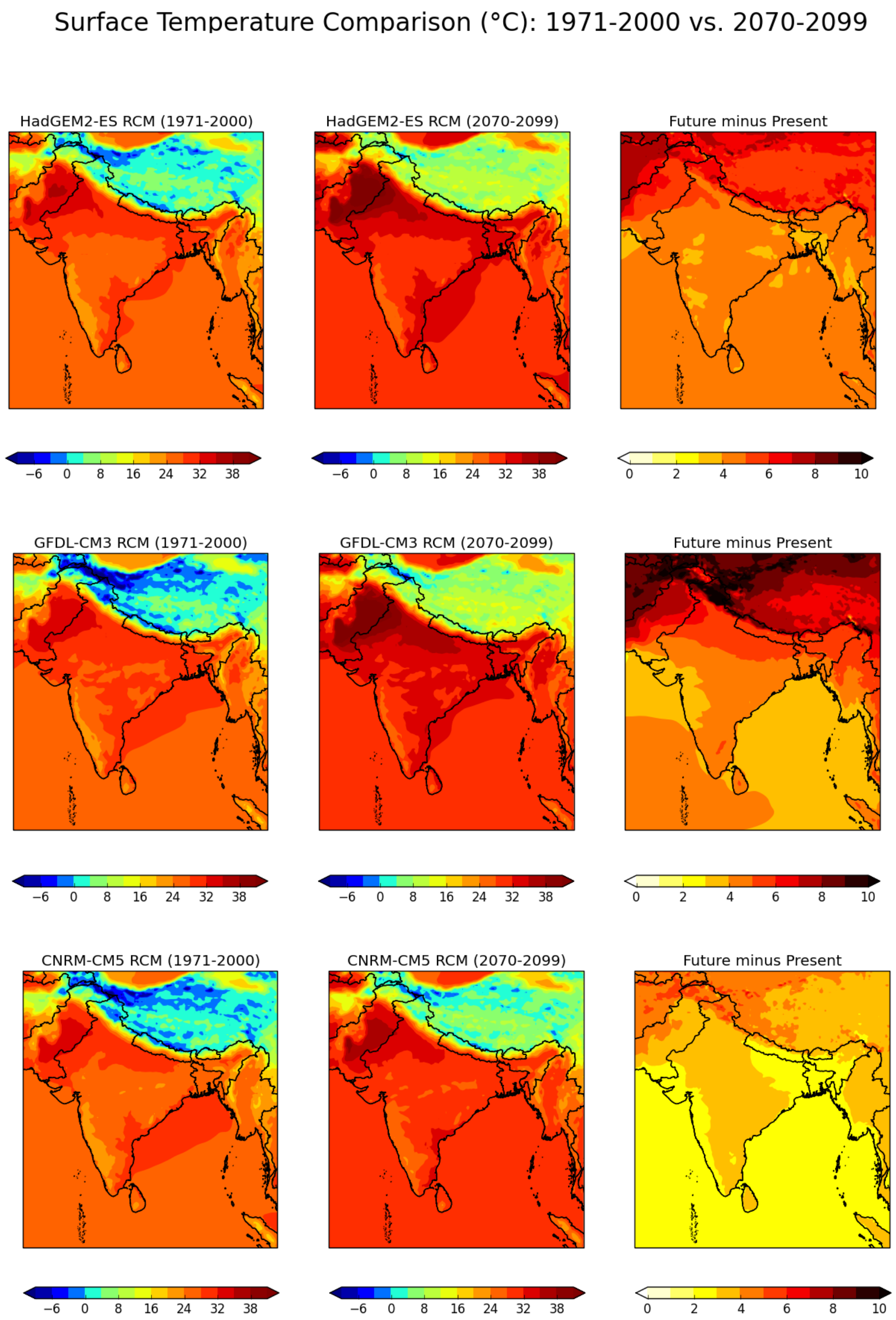

Figure 11: 30-year averaged surface air temperature (°C) during the JJAS season for each of the RCM simulations, spanning 1971-2000 (left column), 2070-2099 (middle column), and the anomaly between the future and present time period (right column).

The HadGEM2-ES-forced simulation projects increases of 3-5° C for most of the region. The greatest increases are in the Himalayas, Pakistan and Eastern Afghanistan. The GFDL-

CM3-forced simulation is the warmest of the three RCM future simulations, especially in the Himalayas/Tibetan Plateau where it projects warming of between 6 and 8°C. For the rest of the region warming is projected to be around 4 to 5°C. The CNRM-CM5-forced simulation gives the least warming of the three RCM future simulations, with warming at only 2-4°C across most of the region. Particularly in the Himalayas, elevation-dependent warming (i.e. where warming is stronger as elevation increases) is a plausible future feedback mechanism under increased global warming, and could lead significant loss of glacial mass balance in the future (Janes & Bush, 2012; Hewitt, 2005; Thomson et al., 2000; Giorgi et al., 1997).

4.2 Precipitation

Figure 12 compares the same time periods as above, but for precipitation during the monsoon season. All three RCM simulations project increases in precipitation and broadly agree in the spatial pattern of the increases, particularly over central India, but vary in their magnitude. The HadGEM2-ES-forced simulation projects increases across the whole region, with the greatest increases of 5-8mm/day along the Western Ghats, in Central India, and over the Bay of Bengal and the Arabian Sea (all areas of intense monsoon rainfall in the present-day climate, playing a large role in the dynamics of the GBM basin). The GFDL-CM3-forced simulation is similar to the HadGEM2-ES RCM, but with greater increases over the Himalayan foothills and slightly lesser increases over the rest of the region. The CNRM-CM5-forced experiment projects the smallest increase of the three RCMs, generally in the range of 2-4mm/day, and the large increases seen over the Bay of Bengal and the Himalayan foothills seen in the other projections are not present. While the magnitudes of increases in monsoon precipitation vary across the RCM models, there is remarkable agreement in the spatial characteristics of these precipitation increases across all three models, which provides a level of confidence that this response is in fact a plausible future climate scenario.

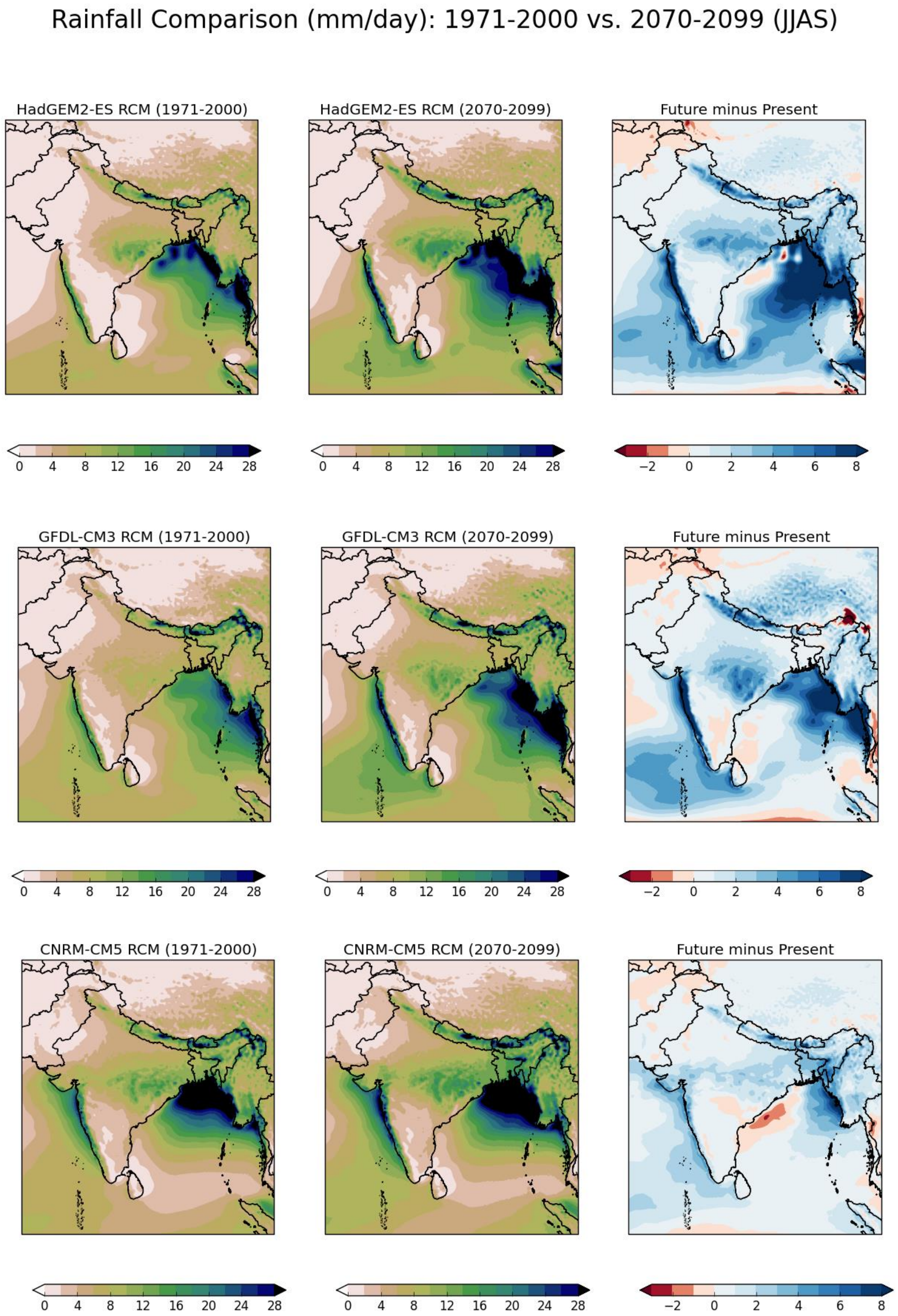

Figure 12: 30-year averaged precipitation (mm/day) during the JJAS season for each of the RCM simulations, spanning 1971-2000 (left column), 2070-2099 (middle column), and the anomaly between the future and present time period (right column).

4.3 Lower-Level Winds (850 hPa)

The spatial extent and magnitude of the precipitation increases projected here are possibly related to a slight strengthening of the monsoon dynamics (Fig 13). As with precipitation, the agreement across all three models for an increase in monsoon circulation strength (albeit with varying magnitudes), provides confidence in the projected large-scale changes in atmospheric dynamics as a plausible future climate scenario. The largest precipitation increases, over central India in particular, come from the GFDL-CM3-forced simulation, which also projects the greatest strengthening of the lower-level monsoon jet in the Arabian Sea. On the contrary, the smallest precipitation increases are seen in the CNRM-CM5-forced simulation, which projects less strengthening of this jet.

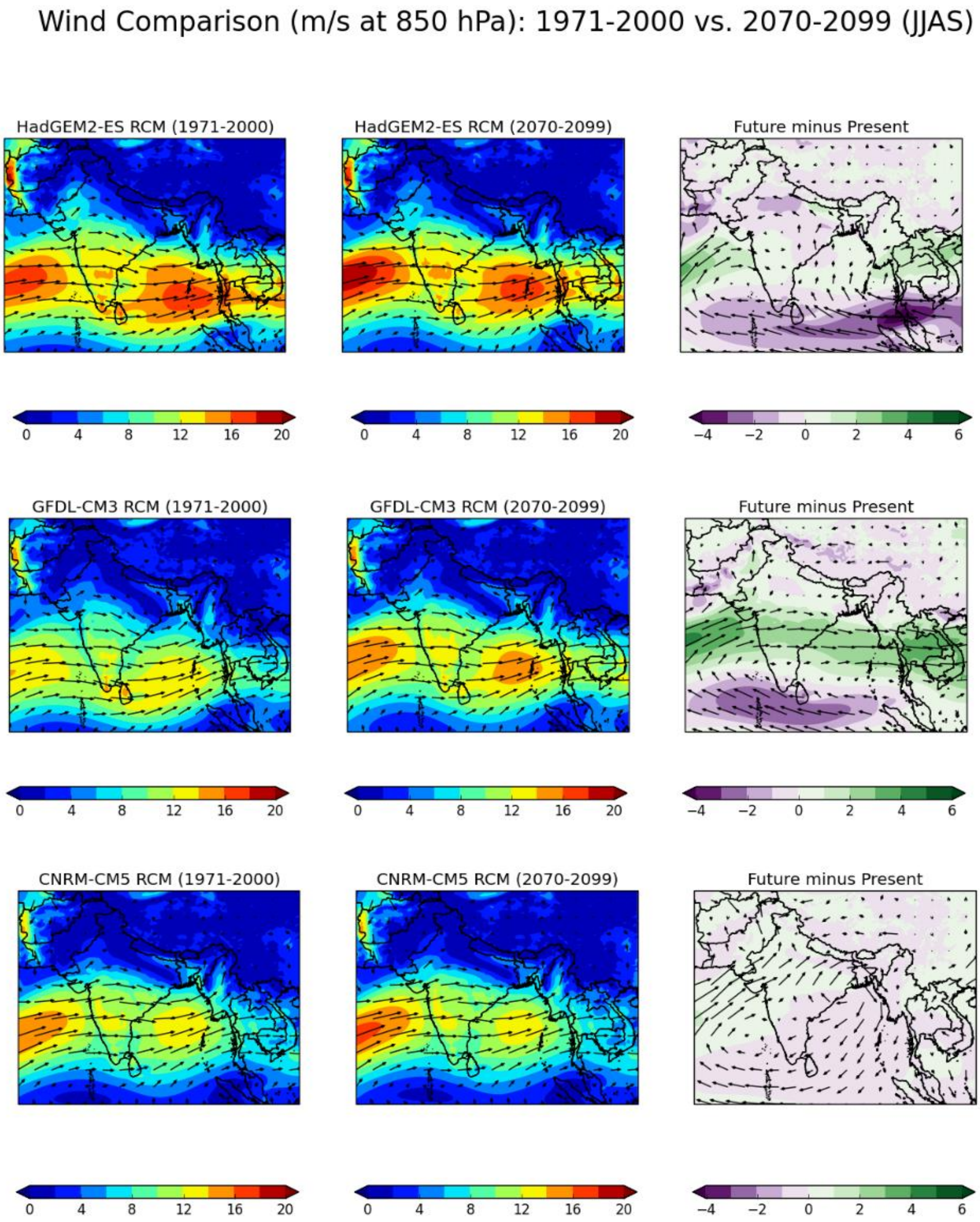

Figure 13: 30-year averaged 850 hPa winds (m/s) during the JJAS season for each of the RCM simulations, spanning 1971-2000 (left column), 2070-2099 (middle column), and the anomaly between the future and present time period (right column).

The seasonally-averaged projections summarised in Section 4 could lead to severe impacts for vulnerable societies located in this monsoon region. With current monsoon heavy precipitation events already resulting in wide-spread flooding and loss of livelihood (for example, the 2017 summer monsoon floods in India, Nepal and Bangladesh), an increased intensity of monsoon-associated rainfall could further exacerbate this risk and, without effective adaptation, could lead to large-scale humanitarian crises (Overpeck & Cole, 2007; O'Brien et al, 2004).

5. EXTREME TEMPERATURE AND PRECIPITATION ANALYSIS

Conditions of extremely hot temperatures have recently been shown to have detrimental impact not just to the economy through lowered crop yields, but to the health and well-being of society as a whole (Lobell et al., 2012; Burgess et al., 2017; Carleton 2017). To assess potential changes in days experiencing extremely hot temperatures within our three RCM simulations, we calculated the TX>35 index, as defined by the Expert Team on Climate Change Detection and Indices (ETCCDI). This index is defined as the number of days in a year that exhibit daily maximum temperatures exceeding 35°C. We calculated the number of days exceeding 35°C for each grid point in our CVA region, then produced climatological averages of these results for the present (1971-2000) and future (2070-2099) time periods. Figure 14 depicts a clear increase in the average number of days exceeding 35°C for all three models, with the largest increases being on the order of 100 days in the GFDL-CM3-forced simulation. Much of these increases are located in regions of intense agricultural activity, such as central and northeast India and central Bangladesh. In addition, increases in the number of extremely hot days in the Himalayan foothills as seen in both the HadGEM2-ES and GFDL-CM3-forced simulations could directly impact river runoff levels, and lead to subsequent governance issues around water and resource management for the densely-populated delta region.

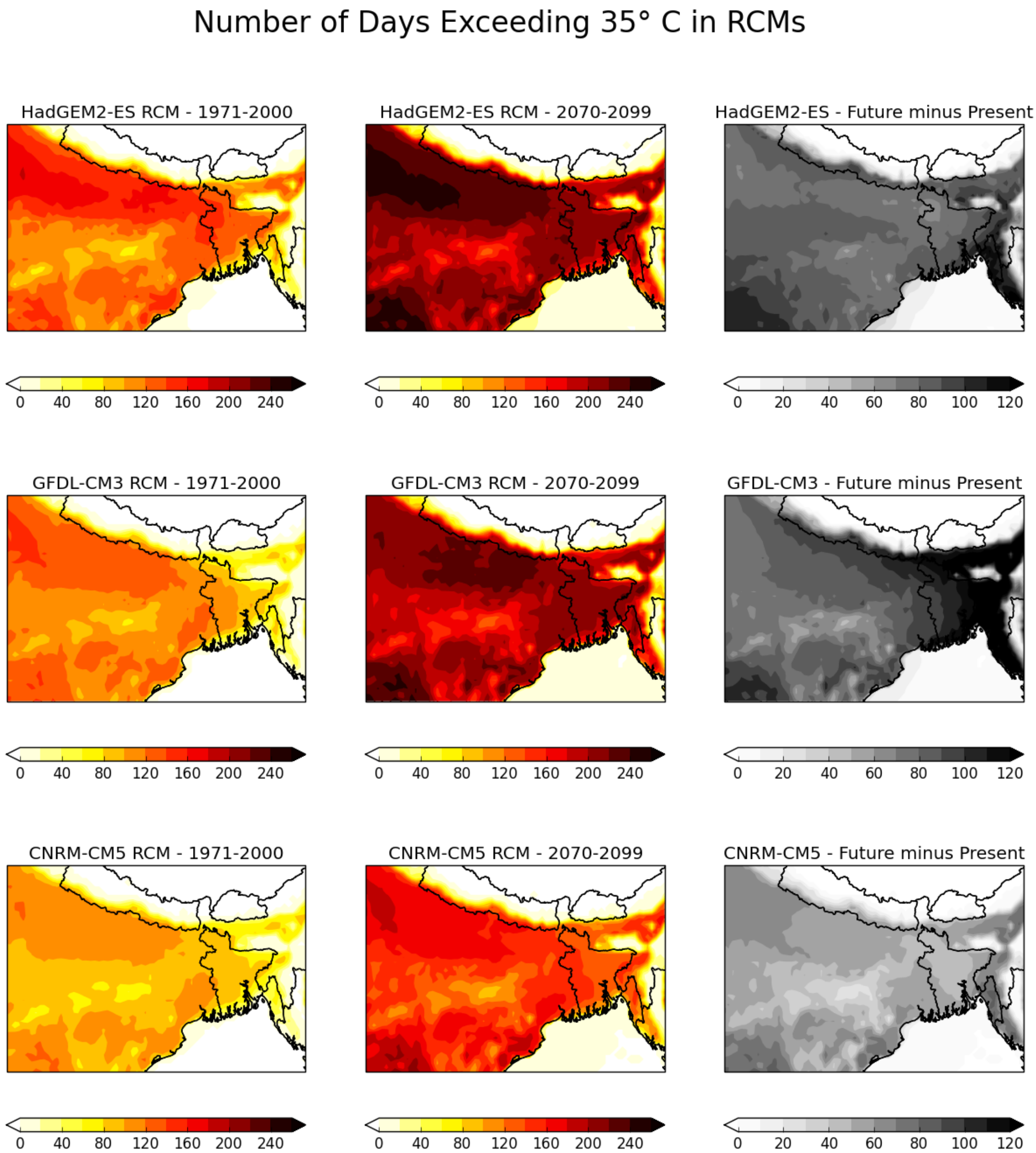

Figure 14: Maps of the TX>35 temperature index (number of days in a year) for each of the RCM simulations (one model per row), across the baseline period of 1971-2000 (left hand column), a future time slice of 2070-2099 (middle column), and the anomaly of future minus present day (right hand column).

As noted above, changes in extreme daily rainfall characteristics could have detrimental impacts on lives, livelihoods and various economic sectors and across South Asia, such as safety and well-being of citizens, water resource management and agricultural productivity.

There are numerous indices describing slightly different aspects of extreme precipitation. To perform an initial investigation of potential changes in extreme daily precipitation, we used the R95pTOT precipitation index, as defined by the Expert Team on Climate Change Detection and Indices (ETCCDI). In this case, R95pTOT was defined as the annual total rainfall which occurs on wet days (when rainfall is > 1 mm/day) that exceed the value of the 95th percentile of rainfall in a baseline period. For each grid point across our CVA region, a 95th percentile value was calculated for wet days in the 1971-2000 period. Then, for a future time period of 2070-2099, we found the annual total rainfall based on days which exceed this baseline threshold at each grid point for each model respectively, such that any projected changes would be with respect to a particular model's own present-day climate. The choice of performing this analysis over the full annual cycle rather than just the JJAS season was to incorporate potential changes in the timing of the monsoon, such that any extreme precipitation days occurring outside the months of JJAS would be accurately captured. A potential change in timing of the monsoon is a topic that has not been thoroughly investigated in this study, but which could occur under increasing greenhouse gas emissions (Ashfaq et al., 2009). The results of this index are shown in Figure 14, which depicts a clear increase in the annual total amount of extremely heavy precipitation across much of the CVA region, particularly over Bangladesh, a signal which is consistent across all three downscaling experiments. An increase in extreme daily precipitation could lead to an increased risk of severe flash-flooding events in a changing climate.

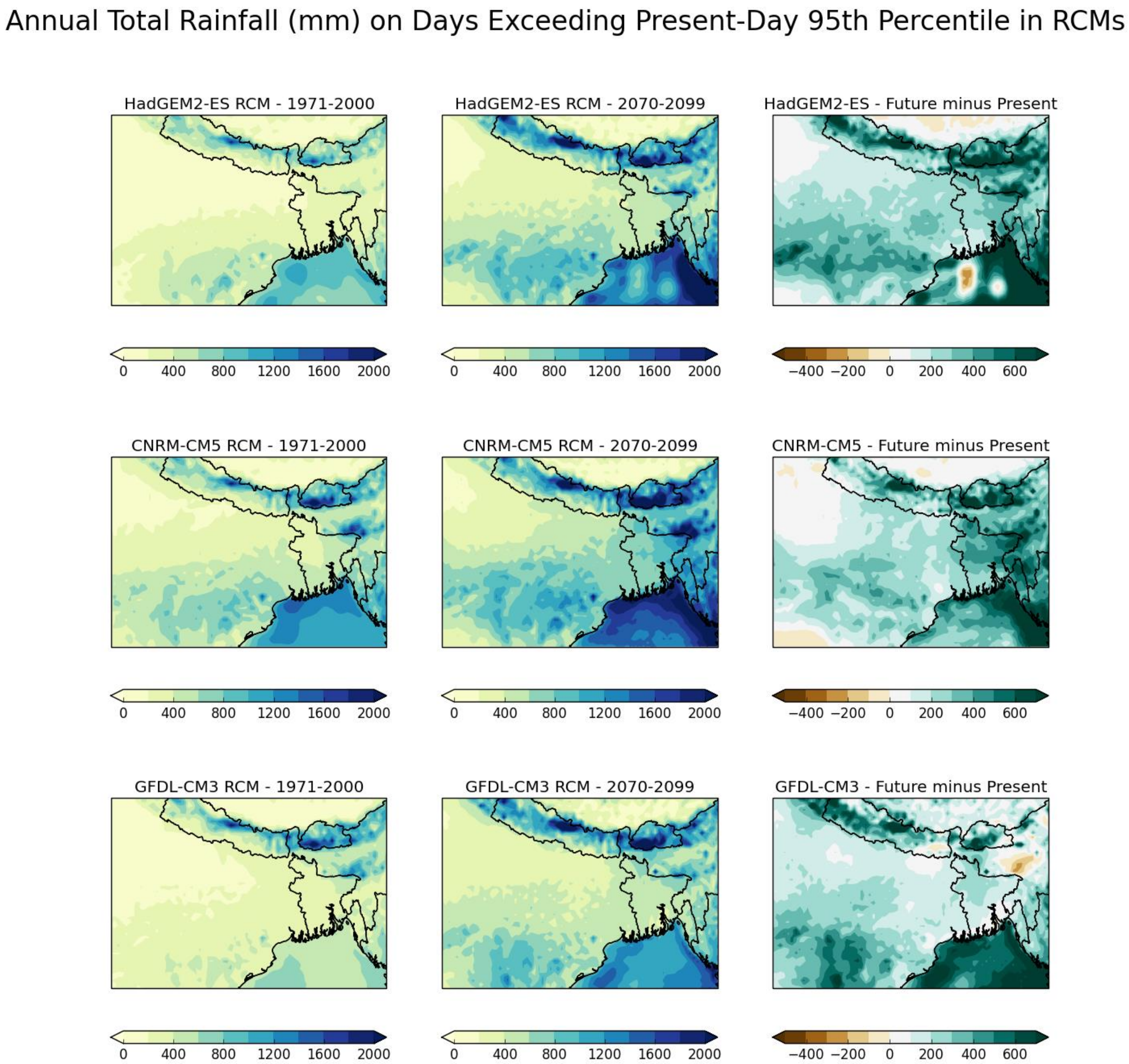

Figure 15: Maps of the R95pTOT rainfall index (number of days in a year) for each of the RCM simulations (one model per row), across the baseline period of 1971-2000 (left hand column), a future time slice of 2070-2099 (middle column), and the anomaly of future minus present day (right hand column).

6. IN THE CONTEXT OF CMIP5

RCM projections found in this study lie within the range of future climate projections simulated by 35 members of the full CMIP5 GCM ensemble for both temperature and precipitation during the monsoon season (Fig 15). These 35 members represent the full CMIP5 ensemble available at the time of analysis. In the case of temperature, the use of an

RCM seems to constrain future projections to span a smaller range than what would have been found by using the driving GCM data alone. On the other hand, precipitation projections using an RCM are seen to span a larger range than the driving GCM data. This could be due to better representation of local topography, and orographic influence on precipitation during the monsoon season. It is worth noting that each of the 35 available CMIP5 models at the time of analysis have been treated with equal weighting. This includes models that may not accurately represent monsoon dynamics and associated precipitation. RCM projections in temperature and precipitation both sit within the range of projections seen in the available CMIP5 ensemble, providing further confidence that the results presented here are not outside the realm of a plausible future climate.

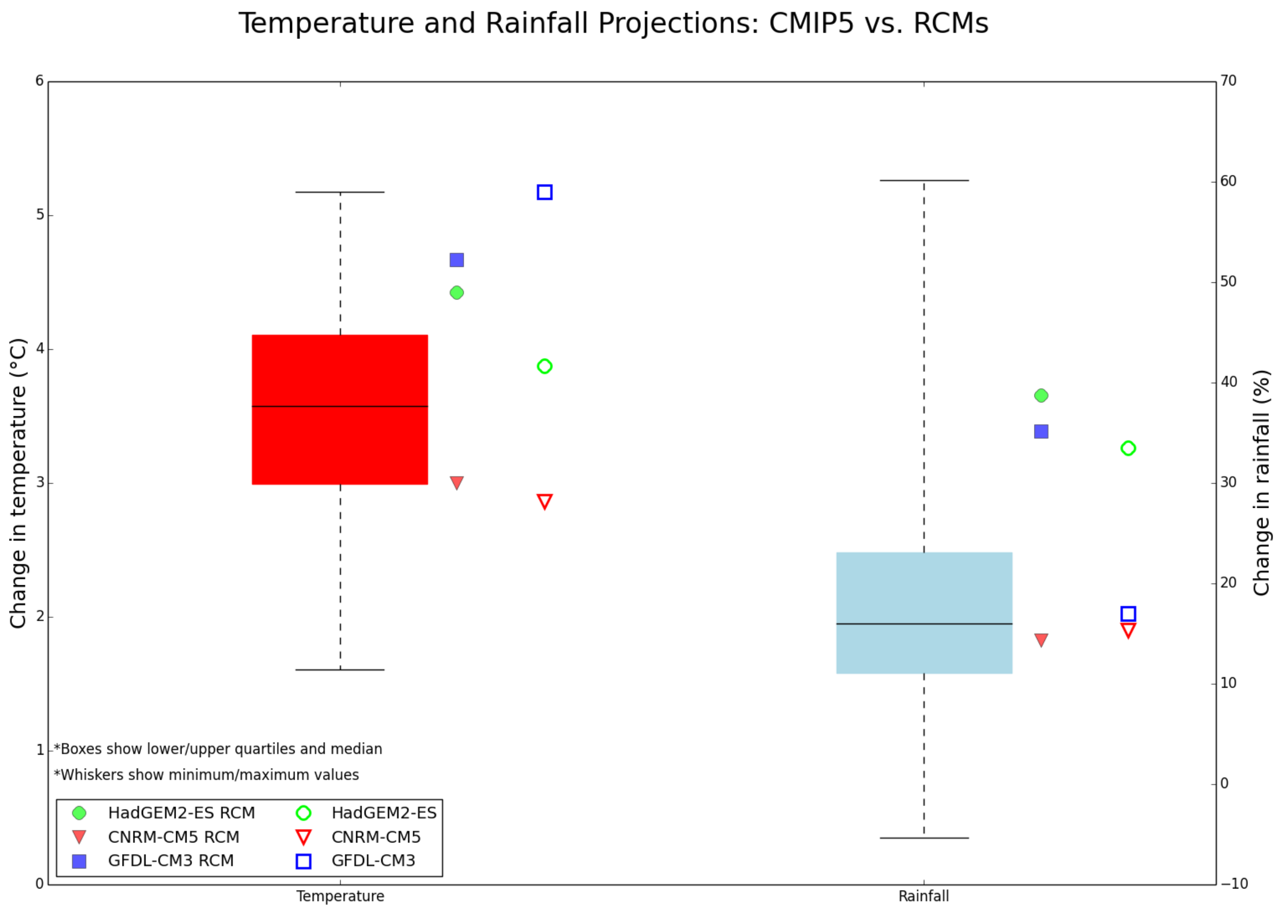

Figure 16: Comparing RCM and GCM anomalies (2070-2099 minus 1971-2000) of temperature and rainfall during the JJAS season to that of the full CMIP5 ensemble under the RCP 8.5 emission scenario. Data have been averaged over the CVA domain in Fig 2. 35

CMIP5 models were available at time of analysis. The lower and upper limit of the boxes depict the 25th and 75th percentile, respectively. The whiskers represent the minimum and maximum values found within the 35 member ensemble.

7. DISCUSSION

There are a number of limitations and uncertainties within the gridded observational datasets used here. Gridded datasets provide improved spatial coverage in areas where spatial and temporal observational stations are sparse (Tozer et al., 2012). They are created through interpolation of station anomalies using a variety of methods, which introduces systematic uncertainties across multiple observational datasets. These datasets are often ‘smoothed’ interpretations of observed point data, and may not capture the spatial and temporal variability of temperature or precipitation in a given region. The sparse station network in South Asia, combined with the presence of complex topography, make it difficult to accurately capture the region’s climate variability in a gridded dataset. For example, it has been shown that, due to a lack of stations in the Himalaya and methods of interpolation used in its creation, the APHRODITE rainfall dataset frequently underestimates the amount of daily rainfall in areas of extreme rainfall and complex topography (Ono & Kazama, 2011; Ali et al., 2012; Menegoz et al., 2013). For South Asia in general, a number of gridded precipitation datasets were compared with station observations gathered by the India Meteorological Department (IMD), all of which showed a large amount of uncertainty across each of the gridded datasets, particularly over Northeast India (Prakash et al., 2014). The use of reanalyses products, such as ERA-Interim, poses an additional challenge as dynamical variables are produced using a model driven by gridded observations, thereby further systematic uncertainties related to model parameterization and set-up. Here, we attempt to limit uncertainties within observational datasets by using multiple sources of information, each employing slightly different methodologies. Given the sparse network of observational stations in this vulnerable part of the world, gridded and reanalyses datasets are a useful and valid tool for understanding current climate variability in South Asia.

Our study focuses solely on the monsoon season of JJAS, as it is during this season when the region receives 70-80% of its total annual rainfall (Caesar et al., 2015; Kumar et al., 2013; Kumar et al., 2006). Results from three RCM simulations over South Asia at a spatial resolution of 25 km have been validated against a range of gridded observational datasets. All three models depict a cold bias over much of the subcontinent, with the strongest cold biases over the Himalayas. As above, this could be due to differences in topography between the model results and observational datasets used for comparison, as well as interpolation methods used to created gridded observational datasets. For precipitation, all three models are slightly too dry during the monsoon season, but too wet in the highest reaches of the Himalayas. This is a known feature of RCM experiments performed in this region, and could be due to how the convective systems and moisture flux into this particularly region is represented (Caesar et al., 2015; Islam et al., 2008). Wet biases in the Himalayas appear to be a common feature of other RCM simulations of the region (Bhaskaran et al., 1996; Ratnam and Kumar, 2005; Das et al., 2006; Saeed et al., 2009), including HadRM3P (Caesar et al., 2015). Some of these apparent wet biases in the Himalayas could be due to underrepresentation of precipitation in the observational data. One contributory factor could be that at high altitudes, “undercatch” of precipitation by rain gauges can be particularly pronounced due to precipitation falling as snow. Some studies have attempted to address this issue by applying undercatch corrections to observational precipitation datasets, and a greater correction is required for snow than for rainfall (e.g. Weedon et al., 2010).

All three RCM experiments, based on the RCP 8.5 emission scenario, depict an increase in seasonally averaged temperature during the monsoon season of JJAS during the 2070-2099 period, ranging from 3-5 °C over central India. All three experiments also indicate an increase in average monsoon precipitation by the end of the century, ranging from 10-40% over central India. While the magnitudes of projected changes vary across the three experiments, spatial patterns remain consistent. This consistency in projections across all three experiments, particularly with regards to the spatial patterns of projected precipitation and atmospheric circulation over the subcontinent, provides a level of confidence in the plausibility of our model projections. A strengthening of monsoon circulation and associated rainfall could lead to detrimental effects in a regional already vulnerable to the impacts of widespread flooding during the monsoon season.

On daily timescales, the total amount of annual precipitation during extremely heavy precipitation days is projected to increase in all three models, potentially leading to an increased risk of severe flooding events in the future. These results are consistent with many previous studies invoking RCM simulations over the Indian subcontinent (Ueda et al., 2006; Krishna Kumar et al., 2011; Kumar et al., 2013).

The RCM simulations undertaken here are similar to those performed by Caesar et al. (2015), the results of which fed into a similar impacts and adaptation project. However, there are key differences between the methods invoked by Caesar et al. (2015) and the methods invoked here. The key contrast between the work performed here and that in Caesar et al (2015) is the use of new, state-of-the-art GCMs within the CMIP5 ensemble for downscaling over South Asia. In addition, the single emission scenario used in Caesar et al. (2015) was the A1B SRES scenario (Nakicenovic et al., 2000). Here, we are implementing a newer approach to modelling emissions based on the RCP emission scenarios (Moss et al., 2010).

There are a number of limitations associated with the research undertaken here, which will have implications for subsequent impact modelling activities. Firstly, due to computational restrictions and modelling capabilities, we have been limited in our selection of driving GCMs to only three models within a small subset of the CMIP5 ensemble. While the three models chosen do span a significant range of uncertainty in future climate projections, the selection of models has an element of subjectivity, and it is possible that choosing different models for downscaling could lead to slightly different results. Uncertainty in RCM responses to identical driving conditions was not explored here, as we chose to use only one RCM for the purpose of this study. However, it is again possible that running multiple RCMs, driven by multiple GCMs, would enhance our ability to provide a more comprehensive range of plausible high resolution projections of climate change over South Asia. This would allow downstream impacts assessments to better inform the range of risks from climate change and how to respond to these. This study was also limited in its scope for assessing changes in extreme climate conditions, such as daily temperature ranges (DTR), consecutive wet/dry days, and monsoon onset/cessation, all of which can have direct and long-lasting impact to many sectors in this vulnerable region. These topics are currently being investigated in follow-on research.

RCM output will contain biases as shown here, some of which will be inherited from the driving GCM and some of which will arise due to characteristics within the RCM itself. Intended users of the RCM outputs must understand the implications of these for their work. How biases are addressed will depend heavily on how the RCM outputs will be used. Climate impact studies can give more plausible results if RCM outputs are statistically corrected towards observations to reduce the effects of biases (e.g. Macadam et al., 2016). However, this is not always possible for biases in all relevant aspects of climate, especially where reliable observations for relevant climate variables are not available. Furthermore, “bias correction” can affect RCM outputs in undesirable ways, such as by modifying climate change signals or the relationships between different climate variables (e.g. Haerter et al., 2011). An alternative approach is to treat the biases as a contribution to uncertainty (Ehret et al. 2012) and interpret the results of downstream impact modelling accordingly.

8. CONCLUSIONS

Results from the RCM simulations performed here match reasonably well with observational datasets over South Asia, but with notable cold biases (particularly over the Himalayas) and slight dry biases over much of the subcontinent. These biases are an expected outcome of downscaling experiments in this region, and do not negatively impact the usability of information produced here. Simulated changes in temperature and precipitation during the monsoon season presented in this study indicate a high level of consensus for increases in both temperature and precipitation during the monsoon season by the end of the 21st century. These results fall within the plausible range of future climate scenarios predicted by the CMIP5 GCM ensemble, further providing confidence in their use for downstream impacts modelling and adaptation studies. On daily timescales, increases in extreme daily precipitation may occur on a smaller number of days in the future, increasing the risk of severe flooding events in a changing climate.

Further work is possible on a number of topics raised within this paper. A further set of models, using multiple RCP emission scenarios, could be downscaled using an RCM in order to expand the range of plausible future climate scenarios at high-resolutions over South Asia. Subsequent analyses of the model results shown here should focus on potential changes in the timing of the monsoon, as well as large-scale atmospheric processes that can be attributed to local-scale changes in monsoon rainfall.

This study provides an example of good practice in generating future climate data that are suitable for downstream impacts modelling and adaptation studies. Three RCM simulations were performed in this study, each using different driving GCM conditions using the RCP 8.5 greenhouse gas emissions scenario, producing a small ensemble of high-resolution regional climate information at 25km resolution. Although the climate datasets produced have limitations, they provide a firm basis for the assessment of impacts of climate change on the GBM and Mahanadi deltas..

ACKNOWLEDGEMENTS

We acknowledge the World Climate Research Programme's Working Group on Coupled Modelling, which is responsible for CMIP, and we thank the climate modelling groups (listed in Table 1 of this paper) for producing and making available their model output. For CMIP the U.S. Department of Energy's Program for Climate Model Diagnosis and Intercomparison provides coordinating support and led development of software infrastructure in partnership with the Global Organization for Earth System Science Portals.

This work is carried out under the Deltas, vulnerability and Climate Change: Migration and Adaptation (DECCMA) project (IDRC 107642) under the Collaborative Adaptation Research Initiative in Africa and Asia (CARIAA) programme with financial support from the UK Government's Department for international Development (DFID) and the International Development Research Centre (IDRC), Canada. The views expressed in this work are those of the creators and do not necessarily represent those of DFID and IDRC or its Boards of Governors.

The authors would also like to thank Carol McSweeney, Simon Tucker, Simon Wilson, Erasmo Buonomo, Saeed Sadri and Florian Gallo for their assistance in the design and implementation of the RCM experiments and analysis performed here. In addition, the authors would like to thank the reviewers for taking time to apply their expertise to provide many constructive suggestions which helped to improve the clarity and quality of this work.

REFERENCES

Adler, R.F. et al. (2003). The Version 2 Global Precipitation Climatology Project (GPCP) Monthly Precipitation Analysis (1979-Present). *J. Hydrometeor.*, Vol. 4, pp. 1147-1167.

Ashfaq, M., Y. Shi, W-w. Tung, R. J. Trapp, X. Gao, J. S. Pal, N. S. Diffenbaugh (2009). Suppression of south Asian summer monsoon precipitation in the 21st century. *Geophysical Research Letters*, 36, L01704, doi: 10.1029/2008GL036500

Bal, P. K., A. Ramachandran, R. Geetha, B. Bhaskaran, P. Thirumurugan, J. Indumathi, N. Jayanthi (2015). Climate change projections for Tamil Nadu, India: deriving high-resolution climate data by a downscaling approach using PRECIS. *Theor. Appl. Climatol.*, doi: 10.1007/s00704-014-1367-9

Bhaskaran, B., R. G. Jones, J. M. Murphy, M. Noguer (1996). Simulations of the Indian summer monsoon using a nested regional climate model: domain size experiments. *Climate Dynamics*, 12, 573-587.

Bhaskaran, B., A. Ramachandran, R. Jones, W. Moufouma-Okia (2012). Regional climate model applications on sub-regional scales over the Indian monsoon region: The role of domain size on downscaling uncertainty. *J. Geophys. Res.*, 117, doi:10.1029/2012JD179560

Burgess, R., Deschenes, O., Donaldson, D., Greenstone, M. (2017). Weather, Climate Change and Death in India. Working paper (London School of Economics, London). Available at http://www.lse.ac.uk/economics/Assets/Documents/personal-pages/robin-burgess/weather-climate-change-and-death.pdf.

Caesar, J., Janes, T., Lindsay, A., Bhaskaran, B. (2015). Temperature and precipitation projections over Bangladesh and the upstream Ganges, Brahmaputra and Meghna systems. *Environ. Sci.: Proccesses Impacts*, 17(6), pp 1047-1056.

Carleton, T. A. (2017). Crop-damaging temperatures increase suicide rates in India. *PNAS*, 114:8746-8751.

Centella-Artola, A., Taylor, M. A., Bezanilla-Morlot, a., Martinez-Castro, D., Campbell, J. D., Stephenson, t. S., Vichot, A. (2015). Assessing the effect of domain size over the Caribbean region using the PRECIS regional climate model. *Climate Dynamics*, 44:1901-1918.

Christensen, J.H., K. Krishna Kumar, E. Aldrian, S.-I. An, I.F.A. Cavalcanti, M. de Castro, W. Dong, P. Goswami, A. Hall, J.K. Kanyanga, A. Kitoh, J. Kossin, N.-C. Lau, J. Renwick, D.B. Stephenson, S.-P. Xie and T. Zhou (2013): Climate Phenomena and their Relevance for Future Regional Climate Change. In: Climate Change 2013: The Physical Science Basis. Contribution of Working Group I to the Fifth Assessment Report of the Intergovernmental Panel on Climate Change [Stocker, T.F., D. Qin, G.-K. Plattner, M. Tignor, S.K. Allen, J. Boschung, A. Nauels, Y. Xia, V. Bex and P.M. Midgley (eds.)]. Cambridge University Press, Cambridge, United Kingdom and New York, NY, USA.

Das SK, Shekhar MS, Singh GP (2006). Simulation of Indian Summer monsoon circulation and rainfall using RegCM3. *Theor Appl Climatol*, 86:161–72.

Dash, S. K., Jenamani, R. K., Kalsi, S. R., Panda, S. K. (2007). Some evidence of climate change in twentieth-century India. *Climatic Change,* 85:229-321.

Dee, D. P., Uppala, S. M., Simmons, A. J., Berrisford, P., Poli, P., Kobayashi, S., Andrae, U., Balmaseda, M. A., Balsamo, G., Bauer, P., Bechtold, P., Beljaars, A. C. M., van de Berg, L., Bidlot, J., Bormann, N., Delsol, C., Dragani, R., Fuentes, M., Geer, A. J., Haimberger, L., Healy, S. B., Hersbach, H., Hólm, E. V., Isaksen, L., Kållberg, P., Köhler, M., Matricardi, M., McNally, A. P., Monge-Sanz, B. M., Morcrette, J.-J., Park, B.-K., Peubey, C., de Rosnay, P., Tavolato, C., Thépaut, J.-N. and Vitart, F. (2011), The ERA-Interim reanalysis: configuration and performance of the data assimilation system. Q.J.R. Meteorol. Soc., 137: 553–597. doi: 10.1002/qj.828

Deque, M., R. G. Jones, M. Wild, F. Giorgi, J. H. Christensen, D. C. Hassell, P. L. Vidale, B. Rockel, D. Jacob, E. Kjellstrom, M. de Castro, F. Kucharski, B. van den Hurk (2005). Global high resolution versus Limited Area Model climate change projections over Europe: quantifying confidence level from PRUDENCE results. *Climate Dynamics*, DOI: 10.1007/s00382-005-0052-1.

Ehret U, Zehe E, Wulfmeyer W, Warrach-Sagi K, Liebert J. (2012).Should we apply bias correction to global and regional climate model data? *Hydrol. Earth Syst. Sci.* **16**: 3391–3404, doi: 10.5194/hess-16-3391-2012.

Evans, J. P., Ji, F., Lee, C., Smith, P., Argüeso, D., and Fita, L. (2014). A regional climate modelling projection ensemble experiment – NARCliM, *Geoscientific Model Development*, 7(2), 621-629, doi: 10.5194/gmd-7-621-2014.

Fan, U., H. van den Dool (2008). A globally monthly land surface air temperature analysis for 1948-present. *J. Geophys. Res.*, DOI: 10.1029/2007JD008470.

Giorgi, F., J. W. Hurrell, and M. R. Marinucci (1997). Elevation dependency of the surface climate change signal: A model study. *J. Climate*, 10, 288–296.

Goswami, B. N., Venugopal, V., Sengupta, D., Madhusoodanan, M. S., and Xavier, P. K. (2006). Increasing trend of extreme rain events over India in a warming environment. *Science*, 314, 1442–1445.

Gu, H., Wang, G., Yu, Z., Mei, R. (2012). Assessing future climate changes and extremes indicators in east and south Asia using the RegCM4 regional climate model. *Climatic Change*, 114:301-317.

Haerter JO, Hagemann S, Moseley C, Piani C (2011) Climate model bias correction and the role of timescales. Hydrol Earth Syst Sci 15: 1065−1079

Harris, I., P. D. Jones, T. J. Osborn, D. H. Lister (2014). Updated high-resolution grids of monthly climatic observations – the CRU TS3.10 Dataset. *Int. J. Climatol.*, doi: 10.1002/joc.3711.

Herold, N. et al. (2016). How much does it rain over land? *Geophys. Res. Lett.*, Vol. 43, pp. 341–348.

Hewitt, K., (2005). The Karakoram anomaly? Glacier expansion and the ‘elevation effect,’ Karakoram Himalaya. *Mt. Res. Dev*., 25, 332–340

IPCC (2013). Climate Change 2013: The Physical Science Basis. Contribution of Working Group I to the Fifth Assessment Report of the Intergovernmental Panel on Climate Change [Stocker, T.F., D. Qin, G.-K. Plattner, M. Tignor, S.K. Allen, J. Boschung, A. Nauels, Y. Xia, V. Bex and P.M. Midgley (eds.)]. Cambridge University Press, Cambridge, United Kingdom and New York, NY, USA, 1535 pp.

IPCC (2014). Climate Change 2014: Impacts, Adaptation, and Vulnerability. Part A: Global and Sectoral Aspects. Contribution of Working Group II to the Fifth Assessment Report of the Intergovernmental Panel on Climate Change [Field, C.B., V.R. Barros, D.J. Dokken, K.J. Mach, M.D. Mastrandrea, T.E. Bilir, M. Chatterjee, K.L. Ebi, Y.O. Estrada, R.C. Genova, B. Girma, E.S. Kissel, A.N. Levy, S. MacCracken, P.R. Mastrandrea, and L.L.White (eds.)]. Cambridge University Press, Cambridge, United Kingdom and New York, NY, USA, 1132 pp.

Islam, M. N., M. Rauddin, A. U. Ahmed and R. K. Kolli (2008). Calibration of PRECIS in employing future scenarios in Bangladesh. *Int. J. Climatol.*, 28, 617–628.

Islam, S. u., Rehman, N., Sheikh, M. M. (2009). Future change in the frequency of warm and cold spells over Pakistan simulated by the PRECIS regional climate model. *Climatic Change*, 94:35-45.

Jacob D, Bärring L, Christensen OB, Christensen JH, de Castro M, Deque M, et al., (2007). An inter-comparison of regional climate models for Europe: design of the experiments and model performance. *Clim. Change*, 81(1):31–52.

James, R., Washington, R., Jones, R. (2015). Process-based assessment of an ensemble of climate projections for West Africa. *Journal of Geophysical Research: Atmospheres*, 120:1221-1238, doi:10.1002/2014JD022513.

Jones, R. G., M. Noguer, D. C. Hassell, D. Hudson, S. S. Wilson, G. J. Jenkins and J. F. B. Mitchell, (2004). Generating high resolution climate change scenarios using PRECIS, Met Office Hadley Centre, Exeter.

Kebede, A. S., Nicholls, R. J., Allan, A., Arto, I., Cazcarro, I., Fernandes, J. A., Hill, C. T., Hutton, C. W., Kay, S., Lazar, A. N., Macadam, I., Palmer, M., Suckall, N., Tompkins, E. L., Vincent, K., Whitehead, P. W. (2018). Applying the global RCP-SSP-SPA scenario framework at sub-national scale: A multi-scale and participatory scenario approach. *Science of the Total Environment*, 635:659-672.

Kendon, E., R. G. Jones, E. Kjellstrom, J. M. Murphy (2010). Using and Designing GCM-RCM Ensemble Regional Climate Projections. *J. Climate*, 23, 6485-6503.

Kripalani, R. H., J. H. Oh, A. Kulkarni, S. S. Sabade, H. S. Chaudhari (2007). South Asian summer monsoon precipitation variability: Coupled climate model simulations and projections under IPCC AR4. *Theor. Appl. Climatol.*, 90, 133-159, doi: 10.1007/s00704-006-0282-0.

Krishna Kumar, K., Patwardhan, S.K., Kulkarni, A., Kamala, K., Rao, K.K. and Jones, R. (2011). Simulated projections for summer monsoon climate over India by a high-resolution regional climate model (PRECIS). *Current Science*, 101(3), pp.312-326.

Kumar, P., Wiltshire, A., Mathison, C., Asharaf, S., Ahrens, B., Lucas-Picher, P., Christenson, J., Gobiet, A., Saeed, F., Hagermann, S., Jacob, D. (2013). Downscaled climate change projections with uncertainty assessment over India using a high resolution multi-model approach. *Science of the Total Environment*, 468-469, pp S18-S30.

Kumar, K. R., Sahai, A. K., Krishna Kumar, K., Patwardhan, S. K., Mishra, P. K., Revadeker, J. V., Kamala, K., Pant, G. B. (2006). High-resolution climate change scenarios for India for the 21st century. *Current Science,* 90(3), pp 334-345.

Lobell, D. B., Sibley, A., Ortiz-Monasterio, J. I. (2012). Extreme heat effects on wheat senescence in India. *Nature Climate Change*, 2:186-189.

Macadam, I., Argüeso, D., Evans, J. P., Liu, D. L. and Pitman, A. J. (2016). The effect of bias correction and climate model resolution on wheat simulations forced with a regional climate model ensemble. Int. J. Climatol., 36: 4577–4591. doi:10.1002/joc.4653

Marzin, C., et al. (2015), "Singapore's Second National Climate Change Study – Phase 1". http://ccrs.weather.gov.sg/publications-second-National-Climate-Change-Study-Science-Reports.

Massey, N., R. G. Jones, F. E. L. Otto, T. Aina, S. Wilson, J. M. Murphy, D. Hassell, Y. H. Yamazaki and M. R. Allen, (2014). Weather@home: very large ensemble regional climate modelling, *Q. J. R. Meteorol. Soc*., DOI: 10.1002/qj.2455.

McSweeney, C.F., R. G. Jones, R. W. Lee, D. P. Rowell (2015). Selecting CMIP5 GCMs for downscaling over multiple regions, *Clim. Dyn.*, Vol. 44/11, pp 3237–326.

Mearns, L. O., Sain, S., Leung, L. R., Bukovsky, M. S., McGinnis, S., Biner, S., Caya, D., Arritt, R. W., Gutowski, W., Takle, E., Snyder, M., Jones, R. G., Nunes, A. M. B., Tucker, S., Herzmann, D., McDaniel, L., Sloan, L. (2013). Climate change projections of the North American Regional Climate Change Assessment Program (NARCCAP). *Climatic Change*, 120:965-975.Menegoz, M., Gallee, H., Jacobi, H. W. (2013). Precipitation and snow cover in the Himalaya: from reanalysis to regional climate simulations. *Hydrol. Earth Syst. Sci.*, 17:3921-3936.

Moss, R., et al. (2010). The next generation of scenarios for climate change research and assessment, *Nature*, Vol. 463/7282, pp. 747-756, http://dx.doi.org/10.1038/nature08823.

Nakicenovic, N., et al. Special Report on Emissions Scenarios: A Special Report of Working Group III of the Intergovernmental Panel on Climate Change (Cambridge Univ. Press, 2000).

Nicholls, R.J., et al. (2017), "The DECCMA scenario framework: A multi-scale and participatory approach to explore the future migration and adaptation in deltas", DECCMA Working Paper, Deltas, Vulnerability and Climate Change: Migration and Adaptation, IDRC Project Number 107642, www.deccma.com.

O'Brien, K., Leichenko, R., Kelkar, U., Venema, H., Aandahl, G., Tompkins, H., Javed, A., Bhadwal, S., Barg, S., Nygaard, L., West, J. (2004). Mapping vulnerability to multiple stressors: climate change and globalization in India. *Global Environmental Change*, 14:303-313.

Ono, K. & Kazama, S. (2011). Analysis of extreme daily rainfall in southeast Asia with a gridded daily rainfall data set. *Hydro-climatology: Variability and Change*, Proceedings of symposium J-H02 held during IUGG2011 in Melbourne, Australia. 169-175.

Overpeck, J. T. and Cole, J. E. (2007). Lessons from a distant monsoon. *Nature News & Views*, 445:270-271.

Pall, P., Aina, A., Stone, D. A., Stott, P. A., Nozawa, T., Hilberts, A. G. J., Lohmann, D., Allen, M. R. (2011). Anthropogenic greenhouse gas contribution to flood risk in England and Wales in autumn 2000. *Nature*, 470:382-385.

Philip, S., Sparrow, S., Kew, s. F., van der Wiel, K., Wanders, N., Singh, R., Hassan, A., Mohammed, K., Javid, H., Haustein, K., Otto, F. E. L., Hirpa, F., Rimi, R. H., Islam, A. K. M. S., Wallom, D. C. H., van Oldenborgh, G. J. (2018). Attributing the 2017 Bangladesh floods from meteorological and hydrological perspectives. *Hydrol. Earth Syst. Sci.*, https://doi.org/10.5194/hess-2018-379

Philip et al., 2018: Attributing the 2017 Bangladesh floods from meteorological and hydrological perspectives. Hydrol. Earth Syst. Sci. Discuss., https://doi.org/10.5194/hess-2018-379

Prakash, S., Mitra, A. K., Momin, I. M., Rajagopal, E. N., Basu, S., Collins, M., Turner, A. G., Achuta Rao, K., Ashok, K. (2014). Seasonal intercomparison of observational rainfall datasets over India during the southwest monsoon season. *Royal Met. Soc.*, 35: https://doi.org/10.1002/joc.4129

Ratnam JV, Kumar KK. (2005). Sensitivity of the simulated Monsoons of 1987 and 1988 to convective Parameterization Scheme in MM5. *J Climate*, 18:2724–43.

Reichler T, Kim J. (2008). How well do coupled models simulate today's climate? *Bull Am Meteor Soc*, 89(3):303–11.

Riahi, K., Rao, S., Krey, V., Cho, C., Chirkov, V., Fischer, G., Kindermann, G. (2011). RCP 8.5 – A scenario of compariatively high greenhouse gas emissions. *Climatic Change*, 109: 33. https://doi.org/10.1007/s10584-011-0149-y

Rupa Kumar, K., Krishna Kumar, K., Ashrit, R. G., Patwardhan, S. K., Pant, G. B. (2002). Climate Change in India: Observations and model projections. In: Shukla, P. R., Sharma, S. K., Ramana, P. V. (eds) Climate change an India Issues, Concerns and Opportunities, Tata McGraw-Hill Publishing Company Limited, New Delhi.

Rupa Kumar, K., Sahai, A. K., Krishna Kumar, K., Patwardhan, S. K., Mishra, P. K., Revadekar, J. V., Kamala, K., Pant, G. B. (2006). High-resolution climate change scenarios for India for the 21st century. *Current Science*, 90:334-345.

Sabade, S., A. Kulkarni, and R. Kripalani (2011). Projected changes in South Asian summer monsoon by multi-model global warming experiments. *Theor. Appl. Climatol.,* 103, 543–565.

Saeed F, Hagemann S, Jacob D. (2009). Impact of irrigation on the South Asian summer monsoon. *Geophys Res Lett*, 36:L20711. http://dx.doi.org/10.1029/2009GL040625.

Schaller, N., Kay, A. L., Lamb, R., Massey, N. R., van Oldenborgh, G. J., Otto, F. E. L., Sparrow, S. N., Vautard, R., Yiou, P., Bowery, A., Crooks, S. M., Huntingford, C., Ingram, W. J., Jones, R. G., Legg, T., Miller, J., Skeggs, J., Wallom, D., Weisheimer, A., Wilson, S., Stott, P. A., Allen, M. R. (2015). Human influence on climate in the 2014 Southern England winter floods and their impacts. *Nature Climate Change*, doi: 10.1038/nclimate2927.

Schneider, U., Becker, A., Finger, P., Meyer-Christoffer, A., Rudolf, Br., Ziese, M. (2015). GPCC Full Data Reanalysis Version 7.0 at 0.5°: Monthly Land-Surface Precipitation from Rain-Gauges built on GTS-based and Historic Data. DOI: 10.5676/DWD_GPCC/FD_M_V7_050

Sylla, M. B., Giorgi, F., Coppola, E., Mariotti, L. (2012). Uncertainties in daily rainfall over Africa: assessment of gridded observation products and evaluation of a regional climate model simulation. *Royal Met. Soc.*, 33, https://doi.org/10.1002/joc.3551

Tanaka, H. L., N. Ishizaki, D. Nohara (2005). Intercomparison of the intensities and trends of Hadley, Walker and Monsoon Circulations in the Global Warming Projections. SOLA 1: 77-80.

Taylor, K., R. Stouffer, G. Meehl (2012). "An Overview of CMIP5 and the experiment design", *Bull. Amer. Meteor. Soc*, Vol. 93/4, pp. 485-498.

Tozer, C. R., Kiem, A. S., Verdon-Kidd, D. C. (2012). On the uncertainties associated with using gridded rainfall data as a proxy for observed. *Hydrol. Earth Syst. Sci*., 16:1481-1499.

Thompson, L. G., T. Yao, E. Mosley-Thompson, M. E. Davis, K. A. Henderson, and P. N. Lin (2000). A high-resolution millennial record of the south Asian monsoon from Himalayan ice cores. *Science*, 289, 1916–1919.

Ueda, H., A. Iwai, K. Kuwako, and M. E. Hori (2006). Impact of anthropogenic forcing on the Asian summer monsoon as simulated by eight GCMs. *Geophys. Res. Lett*., 33, doi: 10.1029/2005gl025336.

van Vuuren, D.P, E. Kriegler, B. C. O'Neill, K. L. Ebi, K. Riahi, T. R. Carter, J. Edmonds, S. Hallegatte, T. Kram, R. Mathur, H. Winkler (2014). A new scenario framework for climate change research: scenario matrix architecture, *Clim. Change*, Vol. 122, pp. 373–386, http://dx.doi.org/10.1007/s10584-013-0906-1.

Weedon, G.P., et al. (2010). The WATCH forcing data 1958-2001: A meteorological forcing dataset for land surface and hydrological models, WATCH Technical Report No. 22.

Williams, K., Chamberlain, J., Buontempo, C., Bain, C. (2015), Regional climate model performance in the Lake Victoria basin. *Climate Dynamics*, 44:1699-1713.

Willmott, C. J., K. Matsuura (1995). Smart Interpolation of Annually Averaged Air Temperature in the United States.

Xie, P., P.A. Arkin (1997). Global precipitation: A 17-year monthly analysis based on gauge observations, satellite estimates, and numerical model outputs, *Bull. Amer. Meteor. Soc.*, Vol. 78, pp. 2539 – 2558.

Yatagai, A., K. Kamiguchi, O. Arakawa (2012). APHRODITE: Constructing a Long-Term Daily Gridded Precipitation dataset for Asia Based on a Dense Network of Rain Gauges. *BAMS*, https://doi.org/10.1175/BAMS-D-11-00122.1.